

# Engineering Biofunctional Enzyme-Mimics for Catalytic Therapeutics and Diagnostics

Qing Tang, Sujiao Cao, Tian Ma, Xi Xiang, Hongrong Luo,\* Pavel Borovskikh, Raul D. Rodriguez, Quanyi Guo, Li Qiu,\* and Chong Cheng\*

The applications of nanomaterial-based enzyme-mimics (Enz-Ms) in biocatalytically therapeutic and diagnostic fields have attracted extensive attention. The regulation of the biocatalytic performances and biofunctionalities of Enz-Ms are essential research objectives, including the rational design and synthesis of Enz-Ms with desired biofunctional molecules and nanostructures, especially at the level of molecules and even single atoms. Here, this timely progress report provides pivotal advances and comments on recent researches on engineering biofunctional Enz-Ms (BF/Enz-Ms), particularly chemical synthesis, functionalization strategies, and integration of diverse enzyme-mimetic catalytic activities of BF/Enz-Ms. First, the definitions and catalogs of BF/Enz-Ms are briefly introduced. Then, detailed comments and discussions are provided on the fabrication protocols, biocatalytic properties, and therapeutic/diagnostic applications of engineered BF/Enz-Ms via hydrogels, nanogels, metal–organic frameworks, metal–polyphenol networks, covalent–organic frameworks, functional cell membranes, bioactive molecules and polymers, and composites. Finally, the future perspectives and challenges on BF/Enz-Ms are outlined and thoroughly discussed. It is believed that this progress report will give a chemical and material overview on the state-of-the-art designing principles of BF/Enz-Ms, thus further promoting their future developments and prosperities for a wide range of applications.

body as biocatalysts.<sup>[1–2]</sup> This kind of high efficient and powerful catalytic abilities endow them great possibilities to be used as catalysts for biosynthesis,<sup>[2]</sup> indicators for environmental monitoring,<sup>[2,3]</sup> and biological therapeutic agents.<sup>[4–6]</sup> However, their shortcomings, such as variability, high cost, troublesome preparation, and difficulty in recycling, have further limited their applications as biomedicine.<sup>[7,8]</sup> The fast developments of nanotechnology and the deep understanding of catalytic mechanisms make it possible to use catalytically active nanomaterials to prepare “artificial enzymes” to simulate natural enzymes.<sup>[4,9,10]</sup> A large number of nano-systems, constructed from metal,<sup>[11–15]</sup> inorganics,<sup>[16–18]</sup> or organic molecules,<sup>[19,20]</sup> have been reported to show catalytic abilities similar to those of natural enzymes. These biocatalytic nanomaterials have also been defined as enzyme-mimics (Enz-Ms), or nanozymes in some cases,<sup>[21–24]</sup> which have presented promising applications in tumor therapies,<sup>[25]</sup> biosensing,<sup>[26]</sup> antipathogen,<sup>[27]</sup> and wound healing.<sup>[28]</sup> Especially with the fast evolution of synthetic and fabrication methods, the


morphology, composition, and proportion of nanoparticles in Enz-Ms are regulated reasonably and efficiently in recent years.<sup>[29–31]</sup> Not only the constructed types of Enz-Ms increase dramatically, the catalytic mechanisms are also gradually

## 1. Introduction

As an essential participant in the metabolism of organisms, natural enzymes regulate catalytic reactions in the human

Q. Tang, Dr. S. J. Cao, Dr. T. Ma, Dr. X. Xiang, Prof. L. Qiu, Prof. C. Cheng  
College of Polymer Science and Engineering  
State Key Laboratory of Polymer Materials Engineering  
Department of Ultrasound  
West China Hospital  
Sichuan University  
Chengdu 610065, China  
E-mail: qiulihx@scu.edu.cn; cheng@scu.edu.cn,  
chong.cheng@fu-berlin.de

Prof. H. R. Luo  
National Engineering Research Center for Biomaterials  
Sichuan University  
Chengdu 610064, China  
E-mail: hluo@scu.edu.cn

 The ORCID identification number(s) for the author(s) of this article can be found under <https://doi.org/10.1002/adfm.202007475>.

Dr. P. Borovskikh  
Martin-Luther-University Halle-Wittenberg  
Universitätsplatz 10, Halle (Saale) 06108, Germany

Prof. R. D. Rodriguez  
Tomsk Polytechnic University  
Lenina ave. 30, Tomsk 634034, Russia

Prof. Q. Y. Guo  
Chinese PLA General Hospital  
Beijing Key Lab of Regenerative Medicine in Orthopedics  
No. 28 Fuxing Road, Haidian District, Beijing 100853, China

Prof. C. Cheng  
Department of Chemistry and Biochemistry  
Freie Universität Berlin  
Takustrasse 3, Berlin 14195, Germany

DOI: 10.1002/adfm.202007475

studied in detail, which significantly augments the beneficial catalytic bioeffects to meet the growing needs in biomedical applications.

Although significant progress is being made since recent years, the applications of Enz-Ms as biomedical agents still face many challenges. The priority one is finding effective ways to enhance and optimize the biocatalytic performances and biofunctionalities of Enz-Ms in diverse physiological environments. Although some reports indicate that the optimized Enz-Ms has no less catalytic activity than natural enzymes,<sup>[32,33]</sup> the biological functionalities of most Enz-Ms still need to be improved urgently to minimize their dosages and satisfy their biological applications.<sup>[34,35]</sup> Besides, the catalytic behaviors of Enz-Ms are also affected by endogenous environmental factors, such as pH, oxidation conditions, and redox systems;<sup>[36–38]</sup> or exogenous ones, like ultrasound, X-ray and light radiations, and electrochemical stimuli,<sup>[39–42]</sup> which may induce the failure of their biocatalytic activity and stability. Importantly, to mimic the specific metal catalytic centers of natural enzymes, Enz-Ms is often designed using multiple metal atoms doping or complex hybrid structures,<sup>[43,44]</sup> making it very challenging to precisely distinguish their active centers and control their functionality and biocompatibility.<sup>[45]</sup> Therefore, it is essential to accurately regulate these critical factors of Enz-Ms, including size, elemental composition, chemical structures, nanotopography, biological properties, and biosafety.<sup>[46,47]</sup>

Aiming to control these key factors, the essential part is to precisely engineer Enz-Ms and tuning their biofunctionalities, especially at the molecule and even at the single-atom level.<sup>[30,48–50]</sup> To precisely engineer Enz-Ms for different reaction processes, the catalytic activity and selectivity of metal sites must be fully explored and understood by experimental and theoretical methods.<sup>[45]</sup> Meanwhile, for the regulation of their biofunctionality and biosafety, the catalytic Enz-Ms have to be carefully integrated with biofunctional molecules and nanostructures. Appropriate surface coatings or structural modifications can modulate their biological properties by adjusting surface bioactivity, surface charge, exposure of active metals, substances' affinity, etc.<sup>[47,51,52]</sup> Therefore, the rational synthesis, structural design, and biofunctionalization of Enz-Ms by biomacromolecules,<sup>[53,54]</sup> cell membranes,<sup>[55,56]</sup> or organic frameworks<sup>[19,20]</sup> are of great significance to achieve Enz-Ms with combined high catalytic performances and improved biomedical application prospects.

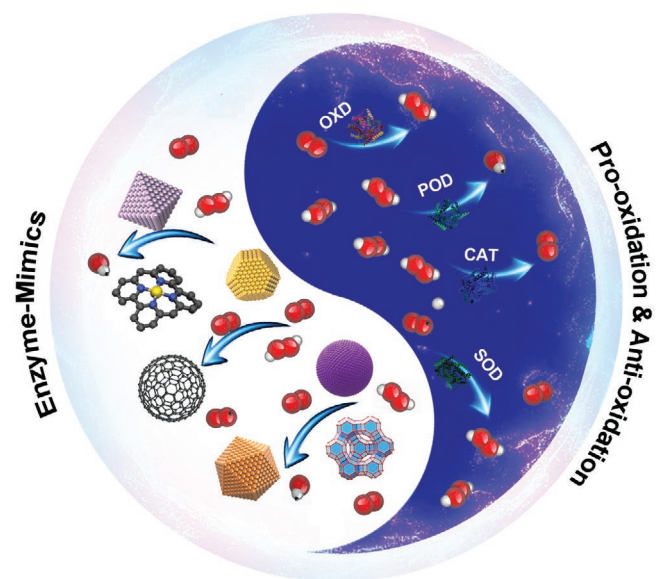
Excellent and comprehensive reviews about how different nanomaterials affect biocatalytic activities and biomedical applications have been introduced, for instance, the design of metal and inorganic nanoparticles-based nanozymes or Enz-Ms.<sup>[35,57–60]</sup> Herein, this timely progress report will especially focus on the recent investigations on engineering biofunctional Enz-Ms (BF/Enz-Ms). Particularly, we focus on the chemical synthesis, functionalization strategies, and integration of diverse enzyme-mimetic catalytic activities of BF/Enz-Ms. First, the definitions and catalogs of BF/Enz-Ms are briefly introduced. Then, we give detailed comments and discussions on the fabrication protocols, biocatalytic properties, and therapeutic/diagnostic applications of engineered BF/Enz-Ms via using hydrogels, nanogels, metal–organic frameworks (MOFs), metal–polyphenol networks (MPNs), covalent organic

frameworks (COFs), functional cell membranes, bioactive molecules and polymers, and composites. Finally, the future perspectives and challenges on BF/Enz-Ms are outlined and thoroughly discussed. We believe that this progress report will provide a chemical and material overview on the state-of-the-art BF/Enz-Ms to understand the designing principles, biocatalytic activities, and bioavailabilities, thus further promoting their future developments and prosperities for a broad range of applications.

## 2. Definitions and Catalogs of Enz-Ms

Enz-Ms, also named as nanozymes in many catalytic nano-systems, which simulates the function of natural enzymes by means of chemical catalysis and nanotechnologies, attract broad interest due to their high biocatalytic efficiency, low cost, and high adjustability.<sup>[22,47,58]</sup> At present, the simulations of natural enzymes by inorganic nanomaterials are mainly concentrated on oxidoreductases as shown in **Scheme 1**, such as the peroxidase (POD), oxidase (OXD), catalase (CAT), and superoxide dismutase (SOD).<sup>[52,57]</sup>

Simulating the bioactivity of natural enzymes using Enz-Ms, generally involves the transfer of electrons and the generation or scavenging of free radicals.<sup>[48,59]</sup> A case in point is the catalytic mechanism of peroxidase-mimics, which belongs to the Fenton or Fenton-like reactions. First, the O–O bond of ROOH gets broken into dihydroxyl radicals after adsorption on the surface of Enz-Ms. Then the intermediate product with colors is formed by partial electron exchange and finally oxidized to CO<sub>2</sub>, H<sub>2</sub>O, or inorganic salts.<sup>[22,47,61]</sup> Generally speaking, the catalytic mechanism of Enz-Ms is similar to that of a natural enzyme. To have a better understanding, the classification of Enz-Ms is commonly done according to the types of natural enzymes, such as the oxidoreductase family and hydrolase family,<sup>[47]</sup> or according to the types of



**Scheme 1.** Illustration of the species of Enz-Ms (or nanozymes in many nanomedicine systems) and their biocatalytic mechanisms for prooxidation and antioxidant.

**Table 1.** The categories of Enz-Ms: classifications, representative materials, and typical applications. ELISA: enzyme-linked immunosorbent assay.

Classifications	Representative materials	Mimetic Enzymes	Applications	Refs.
Inorganics	Carbon Nanomaterials	GO	Glucose sensor	[62,63]
	Semiconductors	Modified g-C <sub>3</sub> N <sub>4</sub>	Glucose oxidase/POD	[64,65]
	Metal oxides	C <sub>60</sub>	SOD	[66,67]
		Metal single-atom catalysts	POD	[68,69]
		Si dots	Horseradish peroxidase	[70,71]
		Se NPs	POD	[72,73]
		MXene	OXD	[74,75]
		MoS <sub>2</sub>	POD	[16,76]
		Black-phosphorus	POD	[77–80]
		Fe <sub>3</sub> O <sub>4</sub>	CAT	[81,82]
		CeO <sub>2</sub>	OXD	[53,83]
		MnO <sub>x</sub>	CAT	[18,84]
		CuO	Horseradish peroxidase	[85]
Metal	Metal nanoparticles (NPs) Metal alloys	Au NPs	Glucose oxidase	[86,87]
		Pt NPs	POD	[88,90]
		Cu NPs	POD	[91,92]
		PdIr	POD	[24,93]
		PtCo	OXD	[94,95]
		PtNi	Horseradish peroxidase	[96,97]
		PtCu	POD	[98,99]
Organics	Organic molecules MOFs COFs	Fluorescein	Glutathione peroxidase	[100,101]
		Polypyrrole	Horseradish peroxidase	[102]
		PEI-DHB	POD	[103]
		Porphyrin	POD	[104,105]
		Pt-MOF	CAT	[106,107]
		Au-MOF	POD/glucose oxidase	[23,108]
		Hemin-MOF	Horseradish peroxidase	[61,109,110]
		FePor-TFPA-COP	POD	[111,112]
		CTF-1	OXD, POD	[113,114]
		Au-COF	POD	[19,115]

catalytically active elements, like iron-based and carbon-based.<sup>[57,60]</sup> Basically, all of these Enz-Ms can be divided into the three categories summarized in **Table 1** according to their material characteristics:

- 1) inorganic nanomaterials, including carbon-based nanomaterials, semiconductors, and metal oxides;
- 2) metals, including metal nanoparticles and metal alloys;
- 3) organics, including small organic molecules, coordination polymers, MOFs, COFs, and other conjugated polymers.

The design of metal, inorganic, and organic materials for Enz-Ms or nanozymes has been recently presented in some excellent and comprehensive reviews as mentioned in the introduction section. Some of the points addressed previously include how different nanomaterials affect biocatalytic activity as well as carefully introducing biomedical applications. Therefore, in the following sections of this review, we will especially focus on the recent findings on using functional molecules and nanostructures to engineer BF/Enz-Ms. The fabrication protocols, biocatalytic properties, and representative biological applications of recently engineered BF/Enz-Ms via using hydrogels, nanogels, MOFs, MPNs, COFs, functional cell membranes, bioactive molecules and polymers, and composites will be discussed sequentially. The structural overview and contents of this review are outlined in **Figure 1**.

### 3. Hydrogel Molecules Engineered BF/Enz-Ms

Hydrogels are 3D, crosslinked networks of water-soluble polymers, which include a wide range of chemical composition and physical properties.<sup>[120–123]</sup> Because of its adjustable physical properties, controllable degradability, and the ability to protect unstable materials from degradation, hydrogels can control the release of various therapeutic agents in spatial and temporal, including small-molecules, macromolecules, nanostructures, and even cells.<sup>[123,124]</sup> Thus, the hydrogel can be used as a platform, where controllable adjustments can be made for drugs/proteins/enzymes delivery or regenerative therapeutics.<sup>[125–128]</sup>

#### 3.1. Porous Hydrogel as the Matrix of Enz-Ms

Porous hydrogels are considered one of the best biomaterials to improve drug transport and interact with cells or tissues because of the large number of pores inside them that can be used as biological metabolites for cargo transport and release.<sup>[129]</sup> In the antibacterial application field, porous hydrogels are widely used in preventing bacterial infections. For example, Sang et al. took advantage of the peroxidase-like activity and near-infrared photothermal properties of MoS<sub>2</sub> to construct an Enz-Ms-hydrogel system with a positively charged and macroporous hydrogel



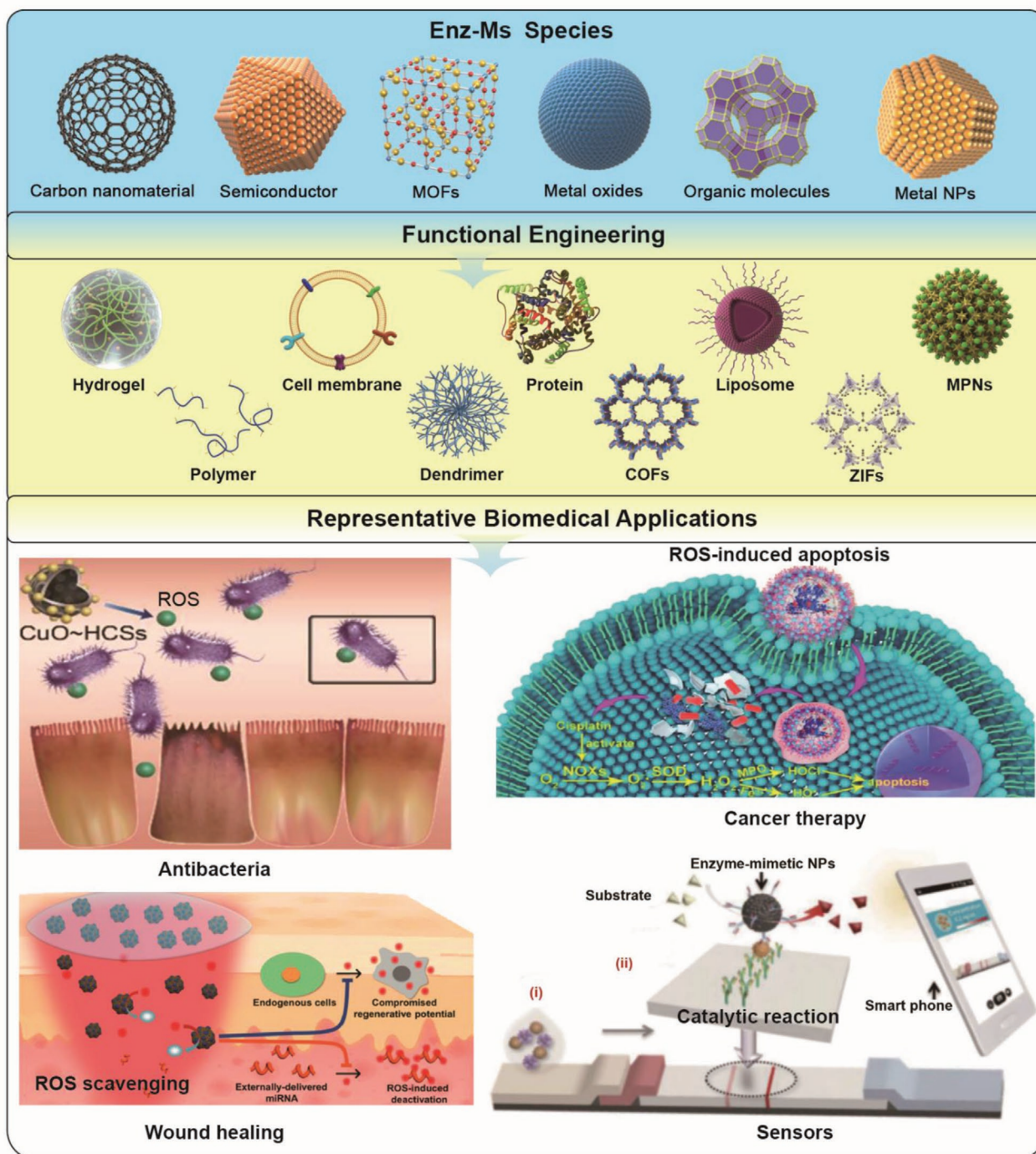


**Figure 1.** Schematic illustration of Enz-Ms species and how they can be engineered by biofunctional molecules and nanostructures for catalytic therapeutics and diagnostics, ROS: reactive oxygen species. Reproduced with permission.<sup>[116–119]</sup> Copyright 2019/2018, American Chemical Society. Copyright 2019, Wiley-VCH.

matrix (Figure 2A-a–d).<sup>[130]</sup> Owing to the positive charge and inner macroporous of the hydrogel, it captured bacteria to enhance the interaction with Enz-Ms, so that the high-density of ROS-induced bacteria-killing happened more effectively in a limited space. It was noteworthy that by combining the near-infrared photothermal and ROS production properties of MoS<sub>2</sub>, the

fabricated Enz-Ms-hydrogels can achieve synergistic bactericidal effects. As shown in Figure 2A-e,f, the near-infrared light (NIR) irradiated and H<sub>2</sub>O<sub>2</sub> stimulated MoS<sub>2</sub>-hydrogel group showed significant bacterial killing abilities. These conditions showed the fastest wound healing promotion by eliminating bacteria and reducing the risk of inflammation.



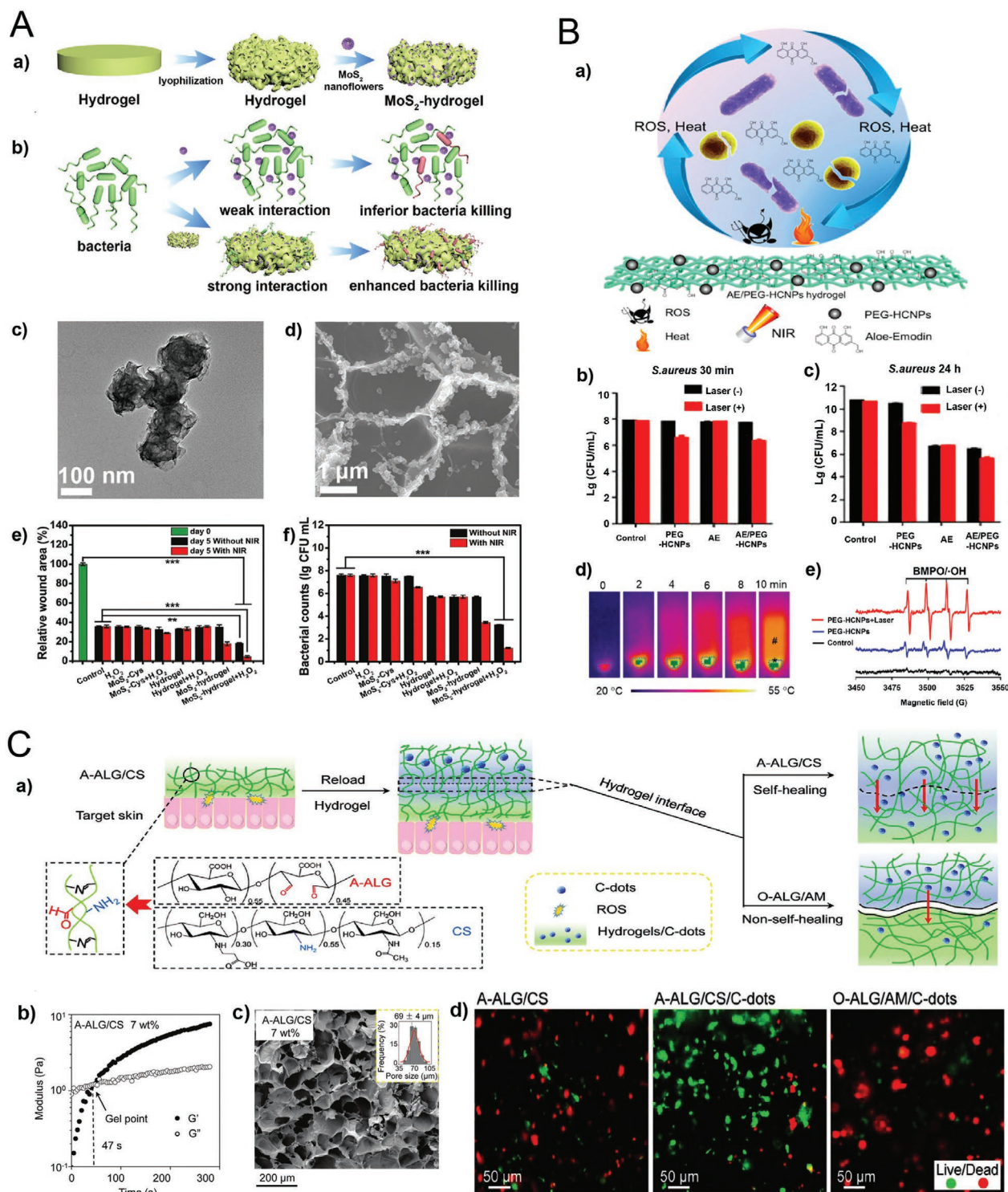


**Figure 2.** A-a) Schematic illustration and b) bacteria-killing mechanism of MoS<sub>2</sub> based Enz-Ms-hydrogel. c) The transmission electron microscopy (TEM) and d) scanning electron microscopy (SEM) images of the MoS<sub>2</sub> based Enz-Ms-hydrogel. e) Relative wound area and f) bacterial numbers of different treatment groups. (\* $p < 0.05$ , \*\* $p < 0.01$ , \*\*\* $p < 0.001$ ). Reproduced with permission.<sup>[130]</sup> Copyright 2019, Wiley-VCH. B-a) Schematic illustration of Aloe-Emodin/carbon nanoparticle hybrid gels. NIR-induced b) short-term and c) long-term antibacterial activities of *S. aureus*. d) Photographs of AE/PEG-HCNP hydrogels with NIR irradiation from 2 to 10 min. e) Electron paramagnetic resonance (EPR) spectra of hydroxyl radicals. (NIR power: 808 nm, 2.5 W cm<sup>-2</sup>). Reproduced with permission.<sup>[131]</sup> Copyright 2018, American Chemical Society. C-a) Schematic illustration of A-ALG/CS hydrogel and its gel-gel transportation of C-dots. b) Gelation time and c) SEM image of A-ALG/CS hydrogel. d) Images of live/dead cell viabilities in different hydrogels. Reproduced with permission.<sup>[133]</sup> Copyright 2019, Wiley-VCH.

Besides using Enz-Ms to kill bacteria directly, the introduction of antibacterial drugs can further deepen the antimicrobial effects. Xi et al. designed a polymer hybrid hydrogel encapsulated with natural antibiotic aloe-emodin and carbon nanoparticles as a new wound dressing against severe skin infections.<sup>[131]</sup> The hybrid hydrogel had two antimicrobial mechanisms: one was the photothermal/ROS pathway triggered by NIR irradiated carbon nanoparticles to release a large number of free radicals and generate heat and high temperature; these effects initially reduced the number of bacteria in a short time (Figure 2B-b–e). The second mechanism was responsible for killing the remaining bacteria by the drug released while turning off the NIR source. Therefore, these two complementary mechanisms together provided excellent long-term antimicrobial properties for various bacteria, including multidrug-resistant bacteria (Figure 2B-a). Moreover, in vivo studies of *Staphylococcus aureus*-infected mice further indicated a promising wound healing ability of this hybrid hydrogel upon NIR irradiation.

In addition to the antibacterial field, the porous hydrogels also show potential applications in regulating pathological microenvironments. Gao et al. recently synthesized a MnO<sub>2</sub> NP-dotted hyaluronic acid hydrogel modified by a synthetic peptide. The hydrogel enables the adhesive growth of mesenchymal stem cells; the MnO<sub>2</sub> NPs can alleviate the oxidative environment to improve the cellular viability of stem cells effectively. Through regulating the toxic microenvironment by scavenging ROS, the MnO<sub>2</sub> NP-dotted hydrogel provides a promising pathway for future stem cell-based therapies in nervous spinal cord tissue regeneration.<sup>[132]</sup>

Shaping the porous structure of the hydrogel system offers an effective way to increase the contact between the drugs and the lesion site. Furthermore, a “dynamic” smart hydrogel system can also be realized by introducing reversible chemical bonds. As a typical example of this, Chen et al. reported a reversible self-repairing porous hydrogel crosslinked by Schiff bases to overcome the diffusive transport of drugs between gel–gel interfaces, named A-ALG/CS hydrogel (Figure 2C-a,c).<sup>[133]</sup> With a gelation time of only 47 s (Figure 2C-b), giving it an effective transport diffusion of the loaded carbon nanodots. Benefited from these advantages, the self-repairing gels loaded with carbon nanodots have better ROS removal efficiency than ordinary gels via using a cell inflammation model (Figure 2C-c), and also show apparent inflammation relief effects.

Furthermore, smart hydrogel systems, including thermosensitive, pH, amylase-responsive hydrogels, and so on,<sup>[134]</sup> can also be used to serve as a versatile matrix to design hybrid Enz-Ms for diverse biomedical applications, such as the localized cancer treatment by injecting hydrogels,<sup>[135]</sup> the oral administration of diabetes using microgels,<sup>[136]</sup> and ROS-responsive polypeptide gel to mediate the concentration of ROS in the tumor microenvironment.<sup>[137]</sup> It is worth noting that except for acting as the matrix of Enz-Ms, the hydrogel itself can also function as a kind of biocatalyst or Enz-Ms since it contains abundant functional groups that can be complexed with metal ions to form a precise 3D structure. For example, the catechol-Fe<sup>3+</sup> coordination hydrogel plays a “Fe-SOD/heme catalases” role to quench various extracellular ROS and promotes the dermal repair of the burn wound.<sup>[138]</sup>

### 3.2. Nanogel Decorated BF/Enz-Ms

Solid hydrogels are a strongly crosslinked network structure with swelling properties in different solvents, including water, buffer solutions, and biological fluids. To further improve its biomedical adaptability, the introduction of microscopic hydrogel gives additional biological properties and enriches its application range.<sup>[139,140]</sup> Nanogels, a kind of hydrogel nanoparticles with a diameter of tens to hundreds of nanometers, are considered to be a multifunctional and feasible platform for biomedical applications, especially in the field of enzymatic catalysis. The nanogel matrix protects the loaded enzymes or biocatalytic nanomaterials from degradation and inactivation and ensures higher cargo loadings and better transport capacity to complete efficient catalysis.<sup>[141–143]</sup>

Wu and his colleagues reported a core (iron oxide nanoparticles)–shell (self-assembled oligopeptides) nanostructured supramolecular hybrid nanogel (SCNGs, Figure 3A-a), which was designed to simulate the nonspecific cytotoxic activities of neutrophil lysosomes via neutrophil-dependent cell inactivation. By co-loading of SOD and chloroperoxidase (CPO) in the nanogel, the conversation of ROS into hypochlorous acid (HOCl) and the following singlet oxygen (<sup>1</sup>O<sub>2</sub>) to destroy tumor cells can be achieved by a cascade reaction. The production of HOCl and <sup>1</sup>O<sub>2</sub> and their time dependence were confirmed by EPR signals, fluorescence intensity test, and fluorescent images (Figure 3A-b–d). Besides, pharmacodynamic tests at both cellular and animal levels have demonstrated <sup>1</sup>O<sub>2</sub>-mediated tumor cell/tissue prolongation inhibition, and this proves that this enzymatic cascade reaction can still be considered effective cancer treatment in the absence of energy activation.<sup>[7]</sup>

In addition to treating tumors, hydrogels are also widely used to promote healing in injured tissues. For wound healing, the formation of functional new blood vessels is crucial. However, for diabetic patients, the neovascularization is usually defective, and the accumulation of ROS is out of control in the diabetic microenvironment, resulting in the difficulty of wound healing. To solve this problem, Wu et al. proposed a special “seed and soil” strategy, which reconstructed the wound microenvironment through cerium oxide (CeO<sub>2</sub>) nanomaterials with redox regulation ability (the “soil”) and wrapped angiogenesis promoted miRNA implants as a “seed” in “self-protection” collagen hydrogel (PCN-miR/Col) (Figure 3B-a–c). Benefiting from the high ROS clearance ability, PCN-miR/Col can not only modify the poor wound microenvironment but also protect the wrapped miRNA from ROS-induced damage. Diabetic wounds treated by PCN-miR/Col showed an apparent acceleration of wound closure and improved wound healing quality (Figure 3B-d–f). Therefore, PCN-miR/Col demonstrates the excellent potential to improve the wound microenvironment and generates new blood vessels with complete functions, providing a new and reliable way for wound healing in diabetic patients.<sup>[117]</sup>

From the above sections, it can be found that both the hydrogels and nanogels working as an ideal matrix not only protect both enzymes and Enz-Ms but also act as reactors for enzyme-catalyzed or enzyme-mimetic reactions to ensure efficient radicals' production. Furthermore, to further advance the application ranges of the hydrogel-modified Enz-Ms, liquid or



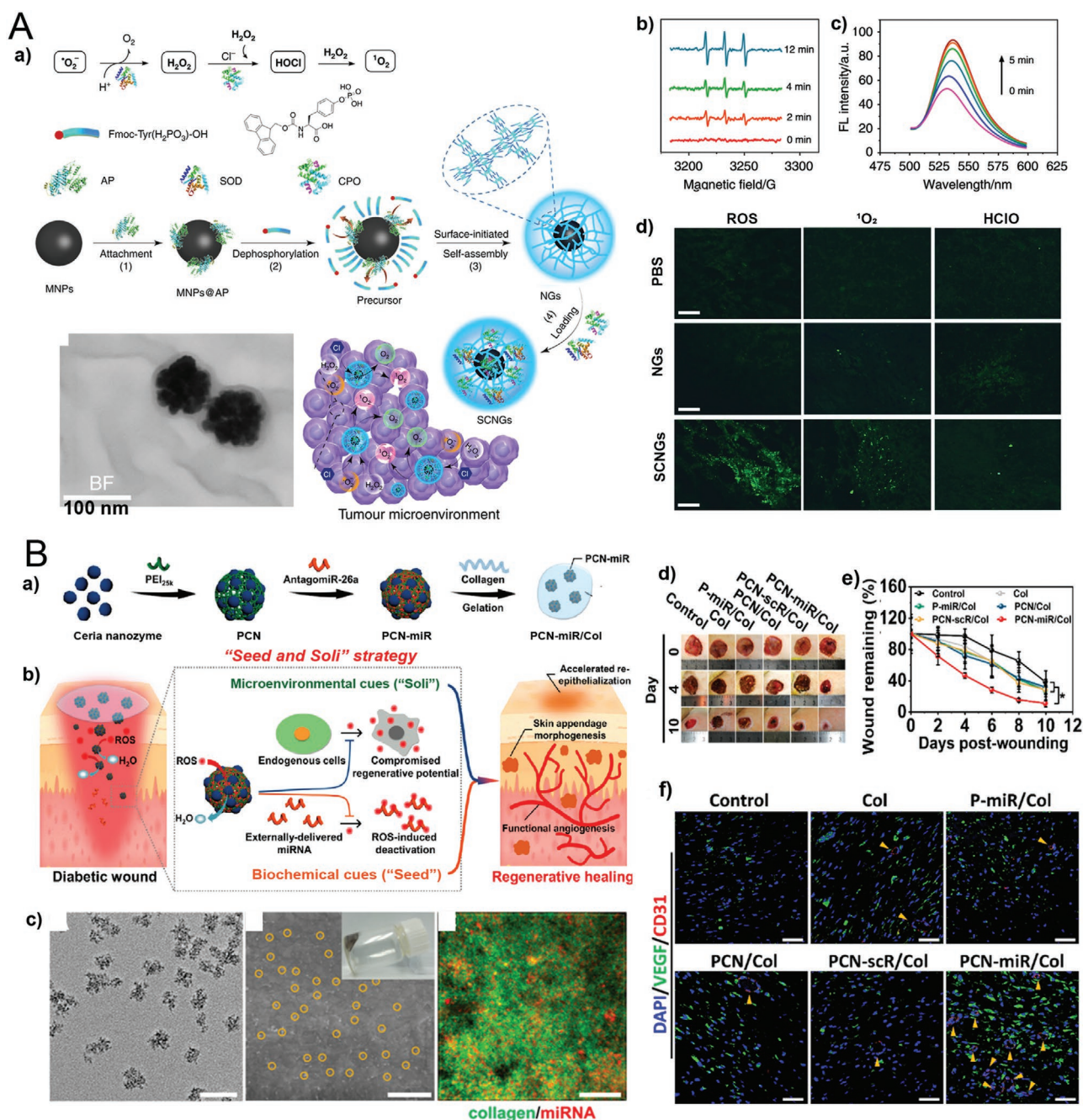


**Figure 3.** A-a) Illustration of the responsive enzyme dynamic therapy mechanism and scan transmission electron microscopy (STEM) image of SCNGs. b) Characterization of the generation of  ${}^1O_2$  and its time-dependence. c) Fluorescence intensity of the singlet oxygen sensor green (SOSG) with SCNGs in PBS buffer ( $20 \times 10^{-3}$  M, pH 6.8). d) Histopathology analysis of ROS,  ${}^1O_2$ , HClO in the hepatocellular carcinoma patient-derived xenograft tumor tissue. Scale bar: 100  $\mu$ m. Reproduced with permission.<sup>[7]</sup> Copyright 2019, Nature Publishing Group. B) Illustration of the a) PCN-miR/Col fabrication. b) PCN-miR/Col-enabled strategy for functional angiogenesis and regenerative diabetic wound healing. c) TEM images of PCN-miR, SEM and CLSM images of PCN-miR/Col, yellow circles represent PCN-miR, green dots represent Col and red dots represent antagomiR-26a. d,e) Images of wounds at day 0, 4, and 10 of healing percentage of wound area ( $n = 5$ ). f) Confocal images of VEGF/CD31 double-stained sections and quantification of numbers. Scale bar: 50  $\mu$ m.  $n = 4$ . f) Photoacoustic images and quantification for oxygenated hemoglobin. Scale bar: 1 mm,  $n = 3$ .  $*p < 0.05$ . Reproduced with permission.<sup>[17]</sup> Copyright 2019, American Chemical Society.

semisolid hydrogel can be introduced to extend the diversities of the matrix. Meanwhile, the appropriate and sustainable release of "killing factors" to achieve an excellent therapeutic effect also matters in many therapeutic systems.

#### 4. MOF Engineered BF/Enz-Ms

Due to their precisely designed molecular/atomic-level catalytic centers, high porosity, large surface area, high loading capacity,



and homogeneous 2D/3D porous crystalline materials,<sup>[144]</sup> MOF materials are emerging as one of the most promising materials to design catalysts with rapid and significant developments in the past ten years.<sup>[31,50,145–147]</sup> The application of MOF in BF/Enz-Ms can be classified into three categories, one is MOF itself serving as Enz-Ms, the other is MOF serving as a matrix to load enzymes, and the third one is MOF serving as both a matrix and also an Enz-Ms.<sup>[148]</sup>

As an example of MOF itself serves as an Enz-Ms, Liu and co-workers reported a Cu-MOF with laccase-like activity by using nucleotides as organic ligands with Cu as metal centers (Figure 4A-a).<sup>[149]</sup> They used guanosine 50-monophosphate (GMP), adenosine 50-monophosphate (AMP), and cytidine 50-monophosphate (CMP) as organic ligands. They determined the irreplaceability of Cu, and when the ratio of Cu to nucleotides was 3:4, Cu-MOF showed the highest laccase-like activity. It turns out that guanosine coordination rather than Cu-phosphate binding is behind the origin of this laccase-like activity as depicted in Figure 4A-b. Compared with natural laccase, the Cu/GMP has higher stability even in extreme environments (such as the high salt, high temperature, extreme pH,

etc.). The proposed biofunctional enzyme-mimics hold a promising application potential in biotechnology.

When utilizing MOFs to serve as a highly porous matrix, a series of natural enzymes were immobilized into MOFs with the help of hydrogen bonding, hydrophobic interaction, or van der Waals forces.<sup>[150]</sup> Moreover, regardless of their enzymatic activity, nanoparticles can also be encapsulated into the MOF cavities.<sup>[151]</sup> To take one example, Li et al. reported a Pt nanoparticle encapsulated Zr-MOF network (Pt NP@UiO-66-NH<sub>2</sub>) for detection and clearance of mercury(II) species with high sensitivity and efficiency, especially for Hg<sup>2+</sup> ions (Figure 4B-a).<sup>[152]</sup> This system benefited from the UiO-66-NH<sub>2</sub> matrix high stability in acidic solution as well as the peroxidase-like activities of Pt nanoparticles. Although the peroxidase-like activity of Pt NP@UiO-66-NH<sub>2</sub> was demonstrated by 3,3',5,5'-tetramethylbenzidine (TMB) oxidation (Figure 4B-b), when it came to the detection of mercury-based substances, the competition between Hg<sup>2+</sup> and TMB for Pt nanoparticles decreased its peroxidase-like activities. This particular property allowed it to accurately distinguish and detect the presence of Hg<sup>2+</sup> with a detection limit of  $0.35 \times 10^{-9}$  M (Figure 4B-c).

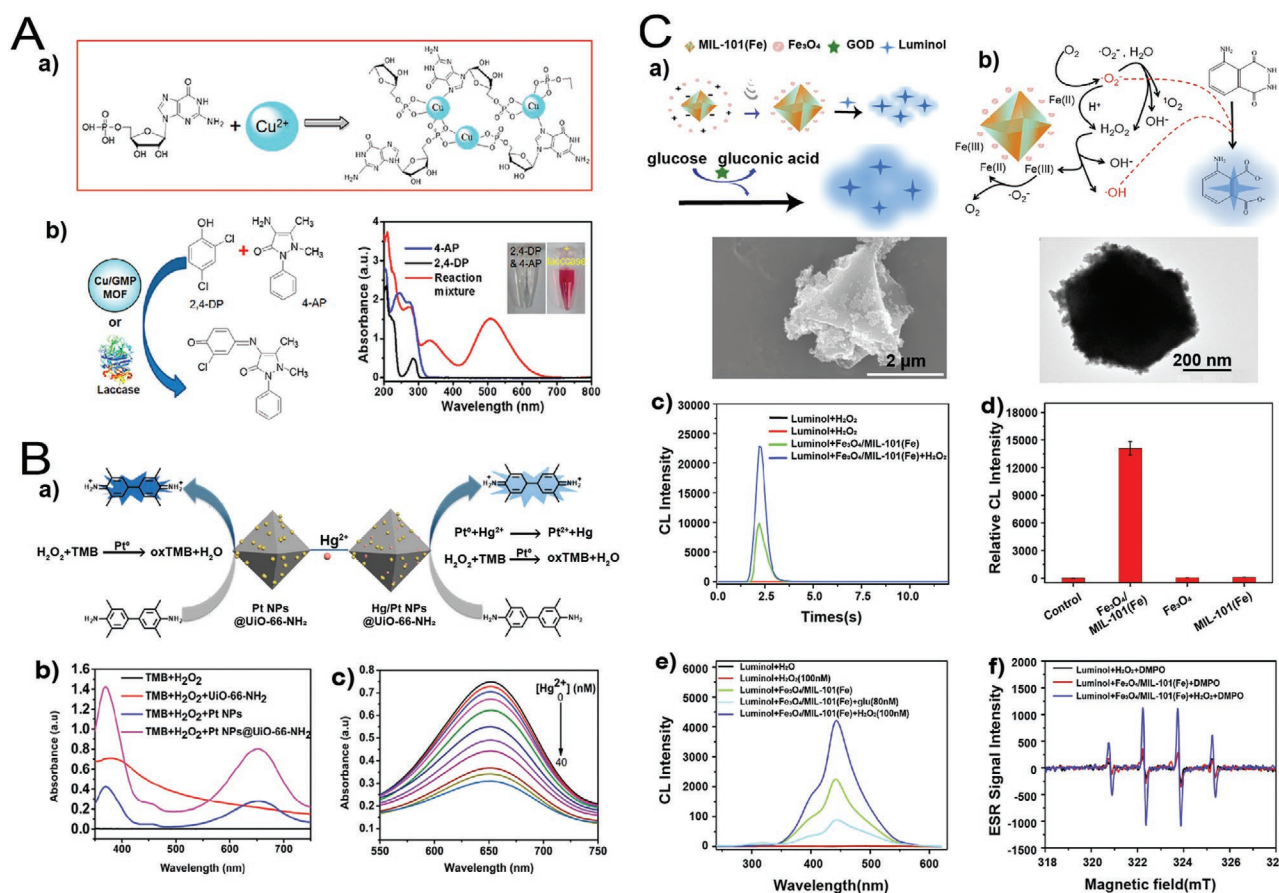


**Figure 4.** A-a) Illustration of Cu-MOF. b) The biocatalytic reaction with Cu/GMP or laccase and UV-vis spectra of 2,4-DP and 4-AP, and their catalytic product. Reproduced with permission.<sup>[149]</sup> Copyright 2017, American Chemical Society. B-a) Illustration of Pt NP@UiO-66-NH<sub>2</sub> and its Hg<sup>2+</sup> capturing ability. b) UV-vis spectra of different TMB oxidized groups and c) Hg<sup>2+</sup> after mixed with Pt NP@UiO-66-NH<sub>2</sub>. Reproduced with permission.<sup>[152]</sup> Copyright 2017, American Chemical Society. C) SEM images and schematic illustration of Fe<sub>3</sub>O<sub>4</sub>/MIL-101(Fe) about a) preparation procedures and b) the mechanism of luminol chemiluminescence (CL). c) Kinetic spectra of luminol CL intensity. Luminol CL intensity of Fe<sub>3</sub>O<sub>4</sub>, MIL-101(Fe), and Fe<sub>3</sub>O<sub>4</sub>/MIL-101(Fe) d) without additional oxidants and e) with H<sub>2</sub>O<sub>2</sub> or glucose. f) <sup>1</sup>O<sub>2</sub> radical detection in different samples. Reproduced with permission.<sup>[156]</sup> Copyright 2017, Elsevier Ltd.

The unique octahedral structure of Pt NP@Uio-66-NH<sub>2</sub> enables its high adsorption capacity for Hg<sup>2+</sup> that was successfully exploited for efficient removal of Hg<sup>2+</sup> in water with an efficiency of over 99%.

Besides the loading of peroxidase-like NPs, integrating ROS-scavenging enzyme-mimetic NPs into the MOF matrix is also very interesting. Qu et al. have developed a straightforward and effective protocol for synergetic neural regeneration by integrating the antioxidative CeO<sub>2</sub> NPs and drugs into MIL-100 simultaneously. This MOF-based nanohybrid exhibits H<sub>2</sub>O<sub>2</sub>-responsive capability to release drugs in the lesion area to enhance the targeted differentiation of neuron cells. Moreover, the integrated CeO<sub>2</sub> endows the nanohybrids with efficient SOD- and CAT-mimetic activities, which can eliminate the ROS and circumvent the oxidative damage of the newly generated neurons, resulting in a longer survival rate and significantly improved neurite outgrowth. These rational-designed ROS-scavenging NPs loaded enzyme-mimetic MOFs nanohybrids exhibit promising application potential in promoting neurogenesis and enhancing the cognitive function in Alzheimer's disease.<sup>[153]</sup>

Moreover, for those MOFs working as both Enz-Ms and matrix, a typical example is the Fe<sub>3</sub>O<sub>4</sub>/MIL-101(Fe) network. Some researchers reported this kind of dual-function MOFs.<sup>[154,155]</sup> Like Tang et al. proposed an ultrasound-assisted electrostatic self-assembled Fe<sub>3</sub>O<sub>4</sub>/MIL-101(Fe) network (Figure 4C-a),<sup>[156]</sup> which was designed to directly catalyze luminol chemiluminescence without additional oxidants. As shown in Figure 4C-c-e, the catalytic activity of Fe<sub>3</sub>O<sub>4</sub>/MIL-101(Fe) was not only 1000-fold stronger than luminol control groups but also significantly stronger than individual Fe<sub>3</sub>O<sub>4</sub> or MIL-101(Fe) groups. Also, the peroxidase activity of Fe<sub>3</sub>O<sub>4</sub>/MIL-101(Fe) was proved by the production of <sup>1</sup>O<sub>2</sub>, so it can be used for ultrasensitive quantitative analysis of H<sub>2</sub>O<sub>2</sub> and glucose with detection limits of  $3.7 \times 10^{-9}$  and  $4.9 \times 10^{-9}$  M, respectively (Figure 4C-f). These nanoparticles loaded MOFs demonstrated the successful detection capabilities of glucose and H<sub>2</sub>O<sub>2</sub> in human serum and medical disinfectants, thereby indicating the application potential of using MOFs-derived BF/Enz-Ms as ultrasensitive detectors for diverse biological fields.

Whether MOFs are used as matrixes or act as biocatalytic mimics,<sup>[157]</sup> their highly controllable bioactivity makes MOFs-based Enz-Ms have great potential for further application in nanomedicines and regenerative therapies.<sup>[158,159]</sup> To improve their biocatalytic efficiency in the biological system, the priority problem to be solved is the difference in optimal catalytic efficiencies between the in vitro pH conditions and the physiological pH environments.<sup>[160]</sup> Based on this, the Qu group designed a MOF-based hybrid nanocatalyst to realize the best catalytic performance through cascade reactions.<sup>[161]</sup> They chose ultrathin 2D MOF (Cu-TCPP (FE)) as the peroxidase model due to its large surface area, which made it easier for the substrate molecules to combine with the active site in a shorter diffusion distance than 3D MOF (Figure 5A-a,b). After integrating glucose oxidase (GOx), the H<sub>2</sub>O<sub>2</sub> and lower pH environments are produced, thus activating the peroxidase activity of 2D Cu-TCPP (Figure 5A-c). The hydroxyl radicals produced by catalysis of H<sub>2</sub>O<sub>2</sub> via 2D Cu-TCPP also proved to have an excellent bacteria-killing ability with high biological safety (Figure 5A-d-f).

In addition to generating ROS, Cu-TCPP can also play a role in removing ROS through reasonable design and matching. For example, Zhang et al. proposed bioinspired Cu-TCPP MOF (CTMDs) nanodots to simulate the SOD enzyme (Figure 5B-a).<sup>[162]</sup> These CTMDs have ultrasmall nanostructures and exhibit high SOD-like activities (Figure 5B-b-d), and the strongest biocatalytic efficiency among all the other tested Enz-Ms (Figure 5B-e-g). Surprisingly, the CTMDs also exhibited glutathione peroxidase (GPx)-like activity (Figure 5B-h); together with its SOD-like ability, CTMDs can clear excess H<sub>2</sub>O<sub>2</sub> and hydroxy radicals at the inflammation sites. The in vitro tests have shown that it can reduce the relative levels of IL-6 and TNF- $\alpha$  in RAW cells (Figure 5B-i), further confirming its ROS scavenging abilities, and also proved to effectively and safely alleviate acute kidney damage caused by lipopolysaccharide (LPS) during endotoxemia.

## 5. MPNs Engineered BF/Enz-Ms

In addition to MOFs, metal-polyphenol based materials, especially the MPNs, also show the potential to serve as Enz-Ms to mediate biomedical treatments. Caruso's group reported the first Fe<sup>3+</sup>-tannic acid coordination complex coating in 2013,<sup>[163]</sup> the MPNs had been recognized as easily prepared and multifunctional platforms both for surface coatings and nanomedicines.<sup>[164–166]</sup> Due to the unique composition of the MPNs, the entire system owns the adhesion abilities of the polyamide or catechol group in the polyphenol substance (phenolic or catecholamine) and also owns the intrinsic catalytic properties of the metal ions themselves.

However, recent studies based on MPNs were mostly using MPNs as carriers or coatings for applications like the clearance of free radicals by phenolic substances,<sup>[167,168]</sup> the characteristics of metal ions themselves are less explored. After the reported of the peroxidase activity of iron nanozymes, various metal ions, including Ce, Mn, V, have also been reported to have free radicals generating abilities via the Fenton-like reaction. Therefore, this unique structure of MPNs also makes it possible to fully utilize the catalytic properties of metal ion centers as Enz-Ms and further expand its application in antitumor fields.

Chen's group proposed a biocompatible MPN-based nanoparticle encapsulated with doxorubicin and platinum prodrug to achieve the enhanced antitumor effects with the combination of nanocatalytic therapy and chemotherapy (Figure 6A-a).<sup>[169]</sup> The simultaneous presence of platinum along with Fe<sup>3+</sup>-polyphenols allows the enzymatic cascade to occur in the following order: first, DOX and platinum prodrugs generate O<sub>2</sub><sup>•−</sup> by activating nicotinamide adenine dinucleotide phosphate oxidase (NOXs), and then convert to H<sub>2</sub>O<sub>2</sub> under the catalysis of SOD-like activity of polyphenols. Finally, highly toxic •OH is produced by the Fenton-like reaction of Fe<sup>3+</sup> and significantly enhance synergistic chemotherapy through a series of biological reactions (Figure 6A-b,c). Besides, they also replaced the DOX with the phagocytic myeloperoxidase (MPO) to obtain a nanoparticle that can produce HOCl in a ROS cascade reaction in situ to enhance the treatment effects of platinum drugs.<sup>[119]</sup> These results indicate that the MPNs based BF/Enz-Ms could act as efficient antitumor therapeutic nanoplateforms.

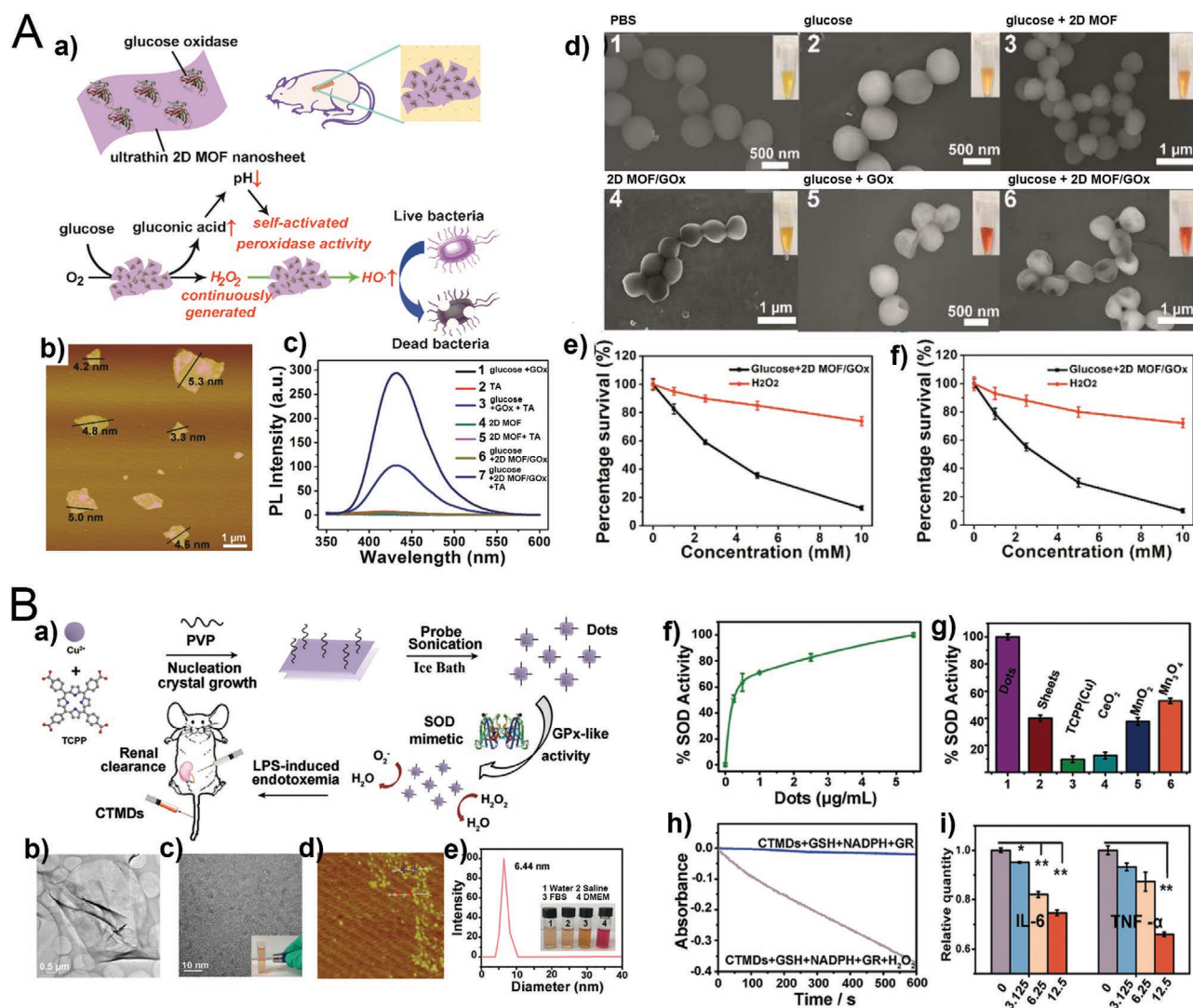


**Figure 5.** A-a) Illustration of the 2D MOF/GOx hybrid nanocatalyst and its antibacterial mechanism. b) AFM image of 2D MOF nanosheets. c) Fluorescence intensity of different samples in PBS buffer (pH = 7.4,  $0.5 \times 10^{-3}$  M) after 12 h. The concentrations of TA, glucose, and 2D MOF/GOx were  $0.5 \times 10^{-3}$  M,  $5 \times 10^{-3}$  M, and  $20 \mu\text{g mL}^{-1}$ , respectively. d) SEM images of *S. aureus* after treated with different groups. The survival rates of e) *E. coli* and f) *S. aureus* treated with H<sub>2</sub>O<sub>2</sub> and glucose + 2D MOF/GOx at different concentrations ( $n = 3$ ). Reproduced with permission.<sup>[161]</sup> Copyright 2019, American Chemical Society. B-a) Schematic illustration of CTMDs. b,c) TEM images of Cu-TCPP nanosheets and CTMDs, inserted: the Tyndall effect of CTMDs in water. d,e) AFM image and diameter of CTMDs. f,g) SOD-like activity of CTMDs and the comparison of SOD-like activity with other Enz-Ms. h) GPx-like activity in the presence of Cu ( $3.5 \text{ mg mL}^{-1}$ ). i) CTMDs induced IL-6 and TNF- $\alpha$  relative quantity of RAW at 3 h with a series of concentrations ( $\text{mg mL}^{-1}$ ). Reproduced with permission.<sup>[162]</sup> Copyright 2019, Royal Society of Chemistry.

Except for the use of chemotherapeutic agents to provide H<sub>2</sub>O<sub>2</sub> via enzymatic cascade as a feedstock for the Fenton-like reaction, the self-supplying H<sub>2</sub>O<sub>2</sub> can also be achieved by encapsulating GOx with a suitable carrier and then coating the MPNs. Therefore, Zhang et al. proposed an ATP-sensitive autocatalytic Fenton-like platform for chemodynamic therapy by incorporating GOx in zeolitic imidazolate framework (ZIF) and then coating with MPNs (GOx@ZIF@MPN) (Figure 6B-a).<sup>[170]</sup> This system degrades the outer shell to Fe<sup>3+</sup> and tannic acid (TA) by overexpressing ATP in tumor cells, thereby producing a large amount of H<sub>2</sub>O<sub>2</sub> by GOx and endogenous glucose, while TA can reduce Fe<sup>3+</sup> to Fe<sup>2+</sup>, followed by Fe<sup>2+</sup> catalysis of H<sub>2</sub>O<sub>2</sub> to generate highly toxic •OH and Fe<sup>3+</sup>, and Fe<sup>3+</sup> can be reduced

to Fe<sup>2+</sup> under the assistance of TA. Thus, as a result, accelerated Fe(III)/Fe(II) cycle conversion and •OH generation are achieved (Figure 6B-b,c), further enhancing the efficacy of Fenton-like reaction mediated therapeutic activities (Figure 6B-d,e).

In the above-mentioned BF/Enz-Ms-based cascade system, the MOFs were proved to show great advantages for cargo storage and protection due to their higher inner space. Another example of this is the construction of p53 plasmid-encapsulated MOF network (MON-p53), which has endowed oxidative stress regulation and Fenton-like reaction to clear tumor cells by ferroptosis/apoptosis hybrid pathway (Figure 6C-a).<sup>[171]</sup> Figure 6C-b,c confirmed the structure of MON-p53 and MON-p53 mediated ferroptosis. Besides, the Fe<sup>2+</sup>/Fe<sup>3+</sup> in the MOF



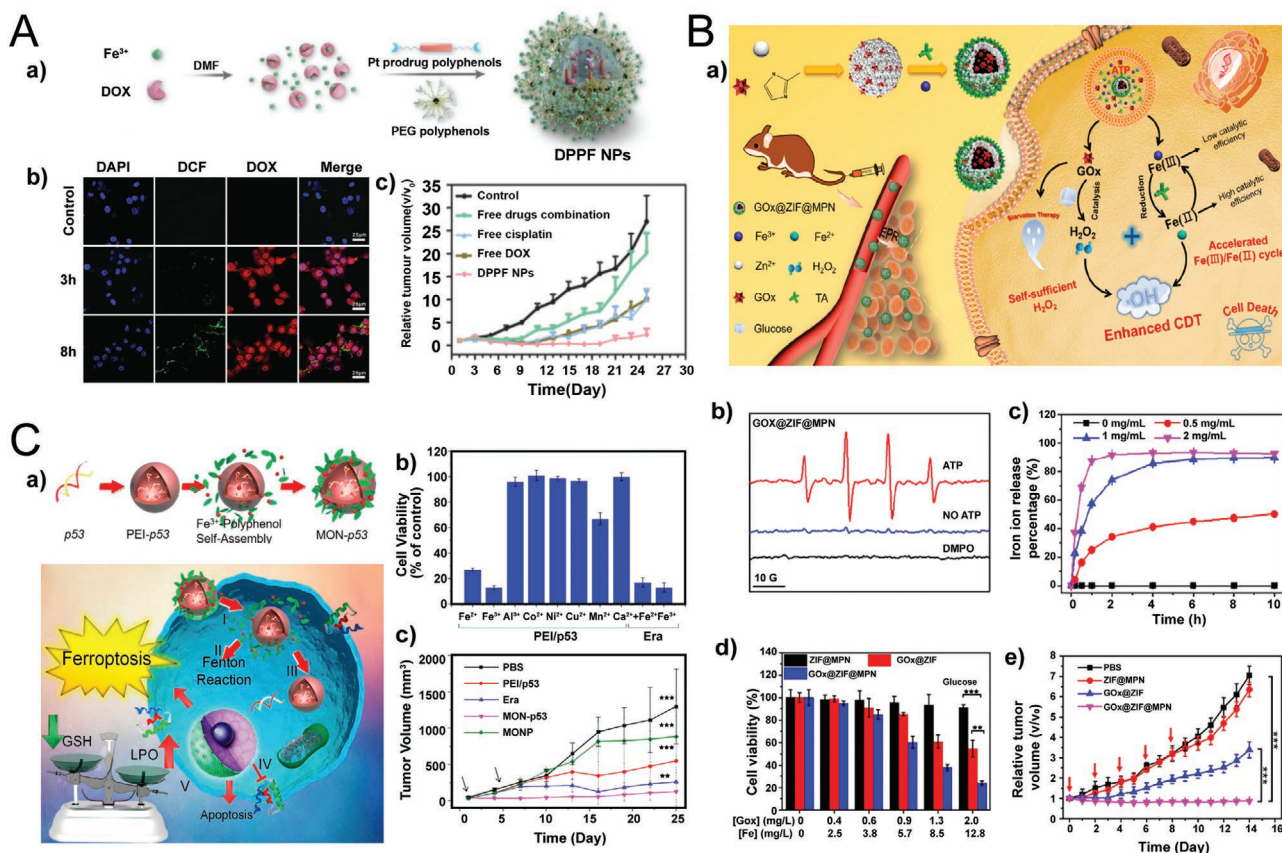


**Figure 6.** A-a) Illustration of the DPPF NPs. b) ROS generation and DOX release from DPPF NPs in U87MG cells at 3 and 8 h. c) Relative tumor volume changes of DPPF NPs, free DOX, free cisplatin, free drug combination, and control group. Reproduced with permission.<sup>[169]</sup> Copyright 2018, Wiley-VCH. B-a) Illustration and mechanism of GOx@ZIF@MPN nanoparticle. b)  $\text{OH}^\bullet$  detection of GOx@ZIF@MPN in the presence and absence of ATP. c)  $\text{Fe}^{3+}$  release from GOx@ZIF@MPN at different ATP concentrations. d) Cell viability of different incubated 4T1 cells in the presence of glucose. e) Relative tumor volume changes of ZIF@MPN, GOx@ZIF, GOx@ZIF@MPN, and PBS group. Reproduced with permission.<sup>[170]</sup> Copyright 2018, American Chemical Society. C-a) Schematic illustration of MON-p53 and its antitumor mechanism. b,c) TEM images of MON-p53 and MON-p53 mediated ferroptosis (p53 concentration:  $2 \mu\text{g mL}^{-1}$ ). d,e) Survival rate and relative tumor volume changes of PBS, PEI/p53, Era, MON-p53, and MONP.  $**p < 0.01$ ,  $***p < 0.001$ . Reproduced with permission.<sup>[171]</sup> Copyright 2017, American Chemical Society.

matrix can further enhance MON-p53-induced ferroptosis compared with other metal ions. What's more, the MON-p53 not only significantly inhibited tumor growth in up to 75 days of in vivo antitumor experiments but effectively prevented the metastasis of tumors into the lungs, liver, and blood (Figure 6C-d,e). These results, therefore, demonstrated that these MPN-based Enz-Ms with ferroptosis/apoptosis-mediated cancer death abilities provide a new illustration of effective cancer treatment.

## 6. COF Engineered BF/Enz-Ms

As a supplement to the porous organic polymer networks (POPs), the COFs exhibited not only high porosity, chemical adjustability, and long-term stability compared with MOFs or MPNs in both aqueous or organic environments.<sup>[172]</sup> Key features such as porosity and crystallinity are essential factors for the immobilization capabilities of natural enzymes; what's more, by introducing suitable metals into COFs, the metal-COF complex structure can also be recognized as enzymatic mimics. For instance, porphyrins have cytochrome-like properties;

however, the porphyrin ring can be easily oxidized and degraded into peroxo-bridged dimers, which make it rapidly deactivated and limit the biocatalytic action of the metalloporphyrin.<sup>[173]</sup> Therefore, the formation of porphyrin-COFs by imine/ borate condensation reactions can not only avoid these disadvantages but also enhance their enzyme-like activity. Some reports show that iron porphyrin-COFs have excellent peroxidase-like activity and can be applied for  $\text{H}_2\text{O}_2$  and glucose detection with sensitivities of  $6.5 \times 10^{-6} \text{ M}$  and  $3 \mu\text{M}$ , respectively.<sup>[107]</sup> Besides, Wu and co-workers reported an iron-porphyrin-based nanocapsule (Fe-TPyP NCs) with multiple peroxidase-like catalytic centers and a  $1.0 \pm 0.1 \text{ nm}$  thickness shell.<sup>[174]</sup> Owing to its hollow structure, this nanocapsule allowed the detection of glucose at concentrations as low as  $0.098 \mu\text{M}$ .

In addition to detecting  $\text{H}_2\text{O}_2$  and glucose, iron porphyrin-COFs can also be used for colorimetric immunoassay of proteins. As shown in Figure 7A-a, Deng et al. reported a pyramidal iron porphyrin-COF (FePor-TFPA-COP), thanks to its porous stereo-structure, large surface area, and multiple surface catalytic centers, which gave it high catalytic activity.<sup>[112]</sup> This system was successfully applied to the enzyme-linked immunosorbent assay

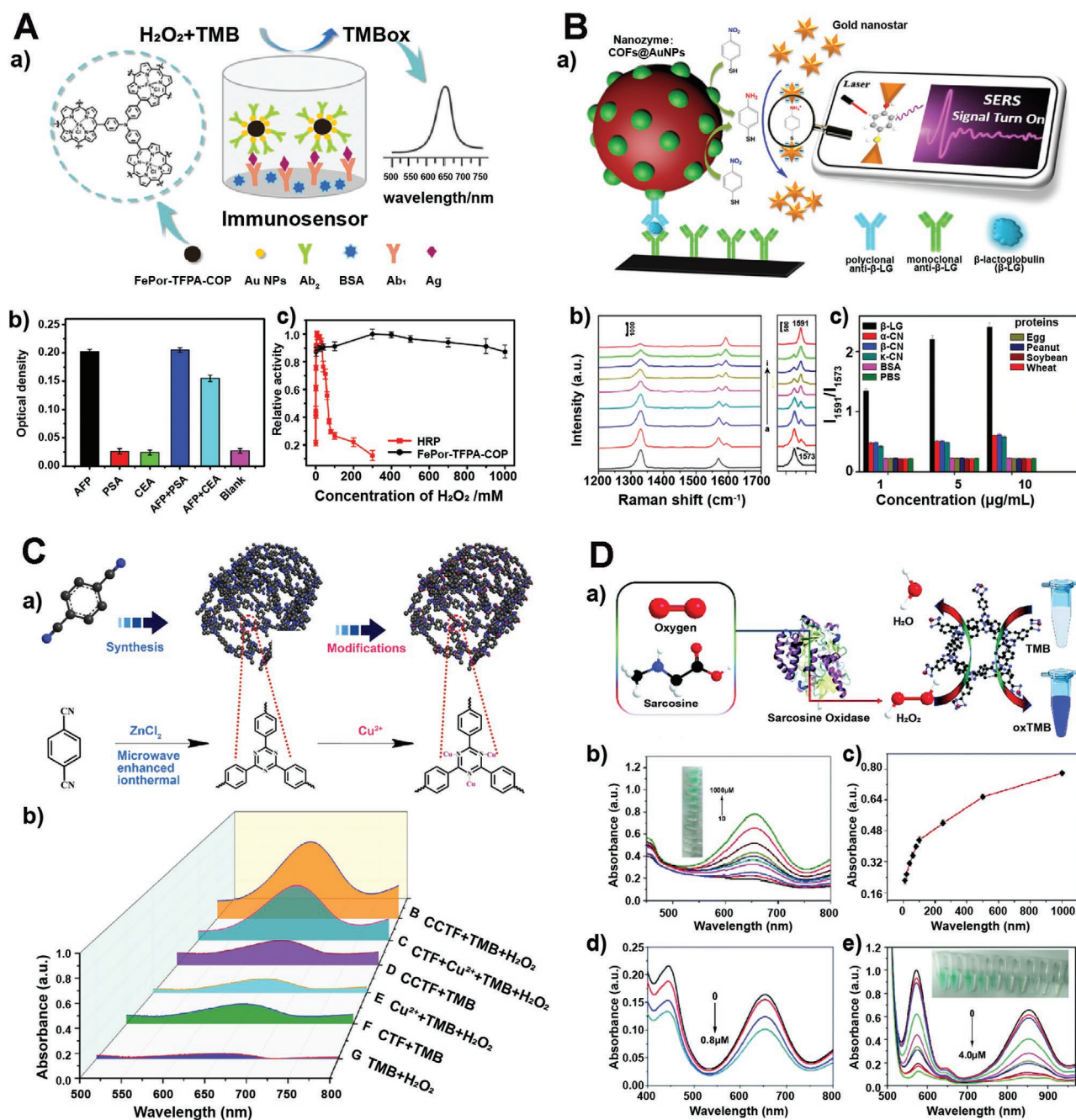


**Figure 7.** A-a) Schematic illustration of FePor-TFPA-COP and its ELISA based detection. b) The specificity of the immunoassay against different kinds of proteins. c) The concentration-relied catalytic activity of FePor-TFPA-COP and HRP. Reproduced with permission.<sup>[112]</sup> Copyright 2017, American Chemical Society. B-a) Schematic illustration of the Au-COF ELISA. b) Changes of 4-NTP's SERS spectra of  $\beta$ -LG from  $1 \times 10^{-3}$  to  $1 \times 10^5$  ng mL<sup>-1</sup>. c) Crossreactivity of the developed Au-COF ELISA with different proteins. Reproduced with permission.<sup>[175]</sup> Copyright 2019, American Chemical Society. C-a) Preparation of the CCTF. b) Adsorption spectra of different catalytic colorimetric reactions. Reproduced with permission.<sup>[176]</sup> Copyright 2017, Wiley-VCH. D: a) Schematic illustration of the sarcosine detection principles. UV-vis absorption spectra of b,c) sarcosine, d) ochratoxin A, and e) fluoride ions. Reproduced with permission.<sup>[114]</sup> Copyright 2018, Royal Society of Chemistry.

(ELISA) detection of  $\alpha$ -fetoprotein (AFP) with a linear response range of 5 pg mL<sup>-1</sup> to 100 ng mL<sup>-1</sup>, a detection limit of 1 pg mL<sup>-1</sup>, and showed excellent stability and reproducibility (Figure 7A-b,c). Therefore, iron porphyrin-COFs have the potential to be highly sensitive and stable bionic catalysts, and further research on their practical applications will also be promoted.

The COF-based ELISA is not limited to iron porphyrin-COFs. Su et al. reported an Au-doped COF system (Au-COF) for ELISA based allergen protein detection (Figure 7B-a).<sup>[175]</sup> They found that Au-COF can convert 4-nitro-thiophenol (4-NTP) into 4-amino-thiophenol (4-ATP), while 4-ATP can efficiently bind to gold nanostars via Au-S bond and electrostatic force to become

a Raman “hot spot.” Therefore, in the surface-enhanced Raman scattering (SERS) detection, the 4-NTP signal ( $1573\text{ cm}^{-1}$ ) will drop, and the 4-ATP will generate a new signal ( $1591\text{ cm}^{-1}$ ). The Au-COF ELISA developed by detecting the ratio between the two signals ( $I_{1591}/I_{1573}$ ) has high-precision detection capability with a detection limit of  $0.01\text{ ng mL}^{-1}$  of numbers of allergens (Figure 7B-b,c).

In addition to the porphyrin-based COFs, another category of COF-based materials that have also been reported to have peroxidase activity in recent years is covalent triazine frameworks (CTFs). CTFs are mimics of peroxidase and oxidase enzymes and capable of catalytic oxidation of chromogenic substrates whether there is  $\text{H}_2\text{O}_2$  or not.<sup>[113]</sup> Besides, Xiong's group reported a Cu-doped CTF structure (CCTF) with robust peroxidase activity against TMB (Figure 7C-a,b).<sup>[176]</sup> Benefiting from the uniform dispersion of  $\text{Cu}^{2+}$  on the surface of CTF, the tunability of the Cu amounts, and the electron-related properties brought by  $\text{Cu}^{2+}$ , CCTF exhibited photoassisted activity as well as high stability and high catalytic properties, and the catalytic ability increases with the increase of  $\text{Cu}^{2+}$ . CCTF had been successfully used for the detection and decomposition of  $\text{H}_2\text{O}_2$  and organic pollutants, which proved that the modification of Cu doping with CTF is an effective method to endow CTF with enzyme-like catalytic activity. Although CCTF is a very attractive new catalytic material, its further applications might be limited because of copper-induced toxicity and large sizes. To improve these shortcomings, the same group proposed a 2D CTF nanosheet using Fe–N as the active center to simulate peroxidase activity (2D-Fe CTF).<sup>[114]</sup> This 2D CTF nanosheet has a larger surface area, better dispersibility, and higher substrate affinity. With the combination of Fe–N atoms, it can provide better catalytic activity than native enzymes and most of the other peroxidase analogs, such as the colorimetric detection of sarcosine, ochratoxin A, and fluoride ions (Figure 7D-a–e). In summary, a variety of COFs and CTFs have been used as BF/Enz-Ms in biosensors, and it is expected that they can also be applied to tumor therapy and other therapeutic aspects if the sizes and morphologies could be well-controlled.

## 7. Cell-Membrane Decorated/Meditated BF/Enz-Ms

Besides, to utilize polymers or biomacromolecules to modify nanocatalytic Enz-Ms to provide better biological properties, another effective method is to encapsulate the Enz-Ms with functional cell membranes and their derivatives.<sup>[177]</sup> The cell membrane extracted by an appropriate method can completely preserve all the complex structures such as lipids, proteins, and carbohydrates; and thus, the membrane-coated materials can possess diverse characteristics and specific biological features exhibited by the cells. Therefore, these cell-mimetic nanosystems have great potential for detoxification, immunomodulation, biological detection, imaging, antitumor, antibacterial, and many other applications.<sup>[177–180]</sup>

### 7.1. Monocytes/Macrophages Meditated BF/Enz-Ms

Owing to the existence of the blood–brain barrier (BBB), the effective treatment of brain-related diseases is an urgent

problem to be solved. Neurodegeneration, such as Alzheimer's disease and Parkinson's disease (PD), share many physiological and biochemical characteristics despite their different manifestations, in which the neuroinflammation caused by the activation of immune cells in the central nervous system is a typical common feature.<sup>[181]</sup> Besides, BBB is decomposed to increase the margin and blood vessels' extravasation during the inflammation process, so that leukocytes can pass through the endothelial cell wall and enter the brain.<sup>[182]</sup> Thus, their abilities to cross the BBB make them ideal cell carriers for drug delivery to the brain.<sup>[183,184]</sup>

Some studies have utilized the above-described pathological properties to design cell-based drug delivery systems. As a very typical example, macrophages are used to deliver gold nanoshells to the brain to treat glioma efficiently.<sup>[185]</sup> Besides taking advantage of enzymes' abilities to alleviate the progression of neurodegenerative diseases, the delivery of enzymes/nanozymes to the neural lesions are also viable solutions.

As a representative example, Batrakova's group established a series of platforms using bone-marrow-derived monocytes (BMM) as carriers to deliver Enz-Ms for PD treatment.<sup>[186–193]</sup> In their studies, they designed various nanoscale enzyme-complexes formed by the assembly of carriers with natural enzymes. By mixing CAT with cationic polymers, the catalytic abilities of CAT can be retained to the greatest extent. They found that this kind of cationic polymers functionalized Enz-Ms can be transported from macrophages through short-term contact between cells or the prolonged formation of pseudopods (filamentous and flaky) to brain microvascular endothelial cells, neurons, and astrocytes efficiently. In the subsequent PD mouse model, they revealed the four possible mechanisms of BMM-mediated therapeutic effects of catalase Enz-Ms in the PD mouse model.<sup>[189–191]</sup> Except for explaining the possible mechanisms, they also designed a layer-by-layer structure for high CAT loading and protected the enzyme from degradation.<sup>[155]</sup>

### 7.2. Tumor Cell Membrane Coated BF/Enz-Ms

Besides macrophages, tumor cell membranes also have been widely used in cell-mimetic nanosystems. Nanoparticles functionalized with cancer cell membranes own the ability of homotypic targeting, which in turn facilitates internalization by tumor cells because of its self-recognition property and thereby allowing self-targeted delivery of different cargo to the tumor tissue.<sup>[195–197]</sup> Because of this, nanoparticles masqueraded with cancer cell membranes can be widely used in anticancer therapies.<sup>[25,198,199]</sup> For example, Li et al. utilized this characteristic by coating the tumor cell membrane on photosensitive  $\text{MnO}_2$ -coated porphyrin Zr-MOF (Figure 8B-a,b), which was loaded with vascular endothelial growth factor receptor 2 and Apatinib, the whole BF/Enz-Ms were named as aMMTm. They also prepared liposome, a HUVEC membrane, and membrane of mouse pancreatic cancer cell line coated nanoparticles. By comparing the in vivo distribution and antitumor effects of these four nanoparticles, it is aMMTm showed the most significant tumor targeting and tumor-killing abilities (Figure 8).<sup>[194]</sup>



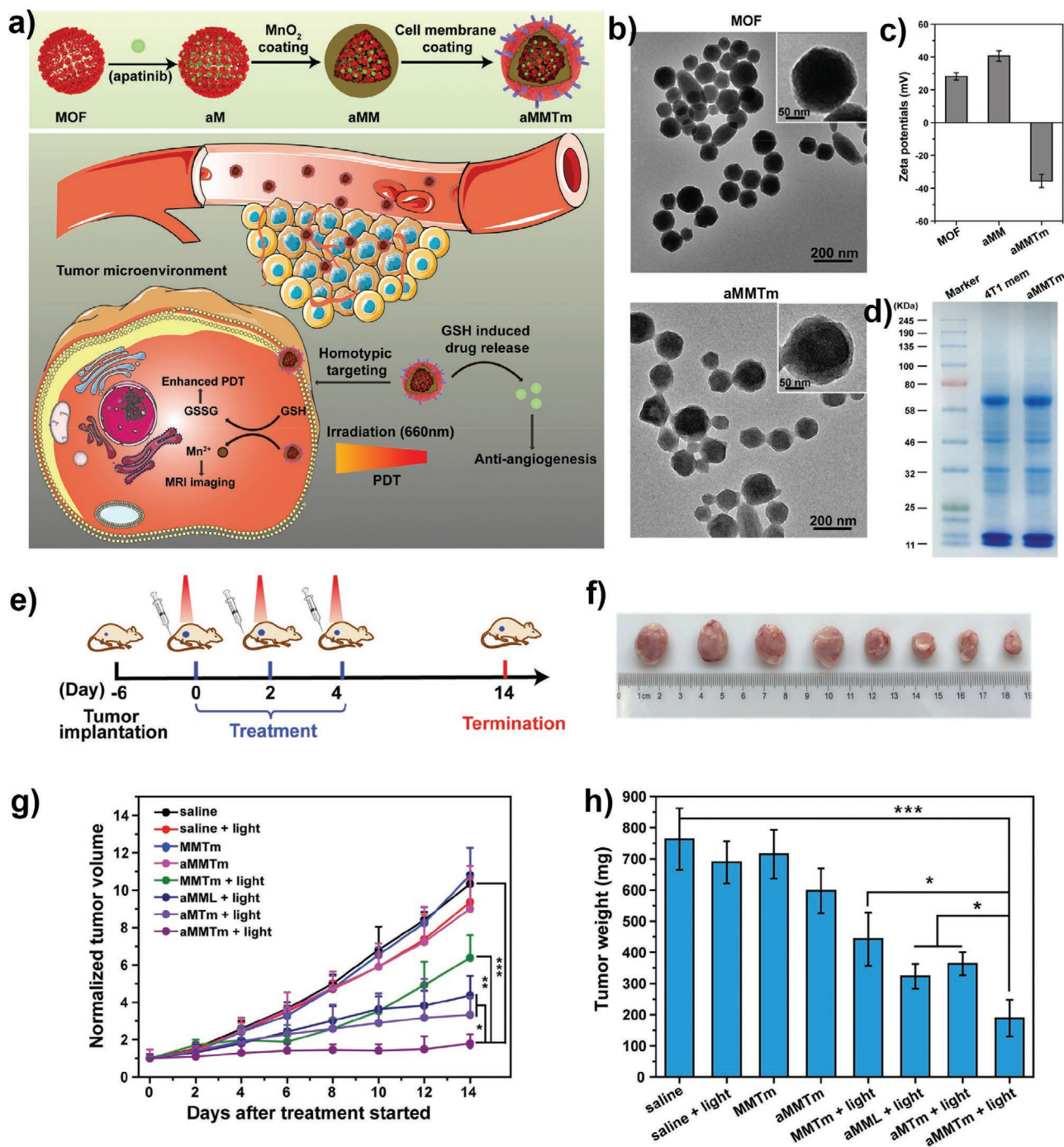


**Figure 8.** a) Illustration of the construction of porphyrinic MOF based aMMTm nanoparticle. b) TEM image of MOF and aMMTm. c) Zeta-potential of the nanoparticles. d) SDS-PAGE analysis of proteins extracted from cell membrane and nanoparticles. e) Schematic image of the in vivo experiment and f) tumor photographs after 14 days. Changes in g) tumor volumes and h) weights of different treated groups over two weeks.  $n = 6$ ,  $*p < 0.05$ ,  $**p < 0.01$ , and  $***p < 0.001$ . Reproduced with permission.<sup>[194]</sup> Copyright 2019, Wiley-VCH.

In addition to chemotherapy drugs, the combination of multiple therapies is also a reasonable means of cancer treatment. It is known that cancer starvation therapy is a very effective treatment by inhibiting tumor growth and proliferation. While photodynamic therapy (PDT) produces ROS in situ, thus

leading to apoptosis or necrosis of tumor cells; or destroying the microvascular circulatory system in tumor tissue, which finally will result in tumor failure as a consequence of hypoxia or nutrient deficiency. Based on this, cascade bioreactors with the combination of cancer starvation and PDT treatments have

been synthesized, such as by coating cancer cell membranes on the GOx and CAT integrated porphyrin MOF (PCN-224), or on the photosensitizers chlorin e6 (Ce6) and GOx coloaded hollow mesoporous silica.<sup>[25,200]</sup> Both nanocascade bioreactors significantly enhanced the production of cytotoxic  $^1\text{O}_2$  under light irradiation. Meanwhile, the cancer cell membrane imparted the biological characteristics of homologous adhesion and immune escape to these BF/Enz-Ms. Therefore, they all exhibited amplifying treatment effects when against cancers, indicating the excellent potential for using in future cancer treatments.

Besides the combination of PDT, there is huge interest to integrate biotherapeutic agents with the MOF nanosystems, for instance the recent Nobel Prize-awarded technology, clustered regularly interspaced short palindromic repeats (CRISPR)-associated 9 (Cas9) system. Khashab reported a kind of nano-biohybrid agent via using human breast adenocarcinoma cell membrane coated CRISPR/Cas9-encapsulated ZIF-8.<sup>[201]</sup> Both the in vitro and in vivo tests demonstrate that this tumor cell membrane coated nano-biohybrid agent exhibit better high cell-targeting ability and better genome editing efficiency, which will inspire future combination of enzyme-mimetic nanoagents with biotherapeutic agents to match the rapidly increased needs for cell-specific targeting treatments.

### 7.3. Red Blood Cell Membrane Camouflaged BF/Enz-Ms

In addition to effectively delivering drugs to the lesion site, the retention time of the nanomedicine in the blood circulation also matters. The immune system, however, can recognize foreign objects. Therefore the traditional nanomedicines are rapidly cleared from the bloodstream by immune cells.<sup>[195,196]</sup> To extend the blood circulation time of nanomedicine, those biomaterials that naturally have a long blood half-life are introduced. Red blood cells (RBCs) express the immunoregulatory marker CD47 on their cell membranes; this transmembrane protein can bind to the inhibitory receptor signaling protein  $\alpha$ , emitting a “do not eat me” signal, inhibiting the phagocytosis of RBCs by immune cells.<sup>[195,196,199]</sup> Therefore, the use of RBCs membrane to camouflage nanoparticles can be used as a biomimetic strategy to prolong the half-life of blood circulation for achieving effective tumor targeting.<sup>[202–204]</sup>

For instance, it was reported that RBCs membrane coated  $\text{MnO}_2$  nanoparticles, which were loaded with GOx and BSA-Ce6, namely rMGB, showed the ability of self-supplying  $\text{H}^+$  and accelerating  $\text{O}_2$  generation (Figure 9A-a).<sup>[205]</sup> rMGB produces  $\text{O}_2$  at the tumor site by catalyzing endogenous  $\text{H}_2\text{O}_2$  and  $\text{H}^+$ , and GOx can utilize  $\text{O}_2$  to consume glucose for cancer starvation treatment. A large amount of  $\text{H}^+$  is produced in the process, which helps to accelerate the  $\text{O}_2$  production of  $\text{MnO}_2$  further, thereby reducing tumor hypoxia and enhancing PDT efficacy (Figure 9A-b–d). Besides, the coating of the RBCs membrane allows rMGB to achieve not only long-circulation effects and sufficient tumor accumulation, but also to avoid systemic toxicity caused by GOx and  $\text{MnO}_2$ .

In addition to using RBCs membrane-encapsulating Enz-Ms alone, the construction of complex biomimetic nanostructures through erythrocyte membranes is also a means of achieving versatile integration. Nie and colleagues reported an “exosome-like”

BF/Enz-Ms,<sup>[203]</sup> which was a folic acid-conjugated, RBCs membrane coated graphene quantum dot Enz-Ms/2, 2'-azino-bis(3-ethylbenzothiazoline-6-sulfonic acid) (ABTS) ABTS nanoparticle (FA-RM: GQDzyme/ABTS) (Figure 9B-a). The FA-RM: GQDzyme/ABTS proved to be bilayer structured nanoparticles with characteristic absorption peaks at 808 nm (Figure 9B-b) and peroxidase activity (Figure 9B-c). This GQDzyme also is a potential candidate for photoacoustic (PA) imaging because in vitro imaging showed that the ultrasound signal at the tumor was 10 times stronger than its counterpart after 8 h of injection (Figure 9B-d). This BF/Enz-Ms systems also exhibited excellent biocompatibility, enhanced cycle time, and improved tumor accumulation in CNE-2 cells (Figure 9B-e). Therefore, it showed the potential to be exploited as a photoacoustic contrast agent for noninvasive nasopharyngeal carcinoma and other types of tumors. Furthermore, some reports proved that Enz-Ms modified by RBCs could be used in carbon monoxide-based gas therapy or sonodynamic therapy,<sup>[206]</sup> illustrating the broad applicability of RBCs modifications.

### 7.4. Cell-Membrane Analogs Meditated BF/Enz-Ms

Liposomes, as analogs of cell membranes, are bilayer hollow vesicles composed of phospholipids with high stability, high biocompatibility, nonimmunogenicity, and biodegradability.<sup>[207,208]</sup> These unique structures enable them to encapsulate hydrophobic and hydrophilic drugs simultaneously, making them attractive drug/Enz-Ms delivery vehicles.<sup>[209,210]</sup> For example, Liu group reported liposomal-based nanoparticles for overcoming tumor hypoxia (Figure 10A-a),<sup>[211]</sup> the ability of CAT@liposome and  $\text{H}_2\text{O}_2$ @liposome to produce  $\text{O}_2$  is demonstrated by staining tissue sections of the tumor, they also induced significant PA imaging signals in the tumor tissue, and the significant increase in oxygenation (Figure 10A-b,c,e). The combination of CAT@liposome and  $\text{H}_2\text{O}_2$ @liposome can significantly improve the therapeutic effect of radiotherapy and provided better biocompatibility and limited toxic side effects (Figure 10A-d). Also, liposomes were reported to functionalize the SOD1-PG-PLL<sub>50</sub> loaded Enz-Ms to treat noninfectious corneal ulcers.<sup>[212]</sup> The obtained results show that this kind of system can reduce the average eye ulcer from  $18.2 \pm 15.1\%$  to  $10.0 \pm 15.0\%$ .<sup>[212,213]</sup>

Another attractive liposomal-like structure is the exosome, a kind of cellular secretory vesicle. The difference between liposome and exosome is the characteristic array of membrane proteins such as tetraspanins on the surface of exosome that endow the immunocompatible ability absent in liposomes.<sup>[214,215]</sup> Thus, exosome-based nanocarriers can escape from the clearance of mononuclear phagocytic systems and function as an “invisibility cloak” to increase the drug transport to the brain. The antioxidant enzyme levels in PD patients are rather low, and natural enzymes, like CAT and SOD, can help to reduce oxidative stress and inhibit neurodegeneration. However, the delivery of CAT across the BBB is a tough challenge, but the use of macrophage secreted exosomes seems a promising solution for delivery in PD therapy. Therefore, Batrakova et al. provided a CAT delivered exosome-based system (exoCAT),<sup>[216]</sup> they studied the difference of various preparation methods of



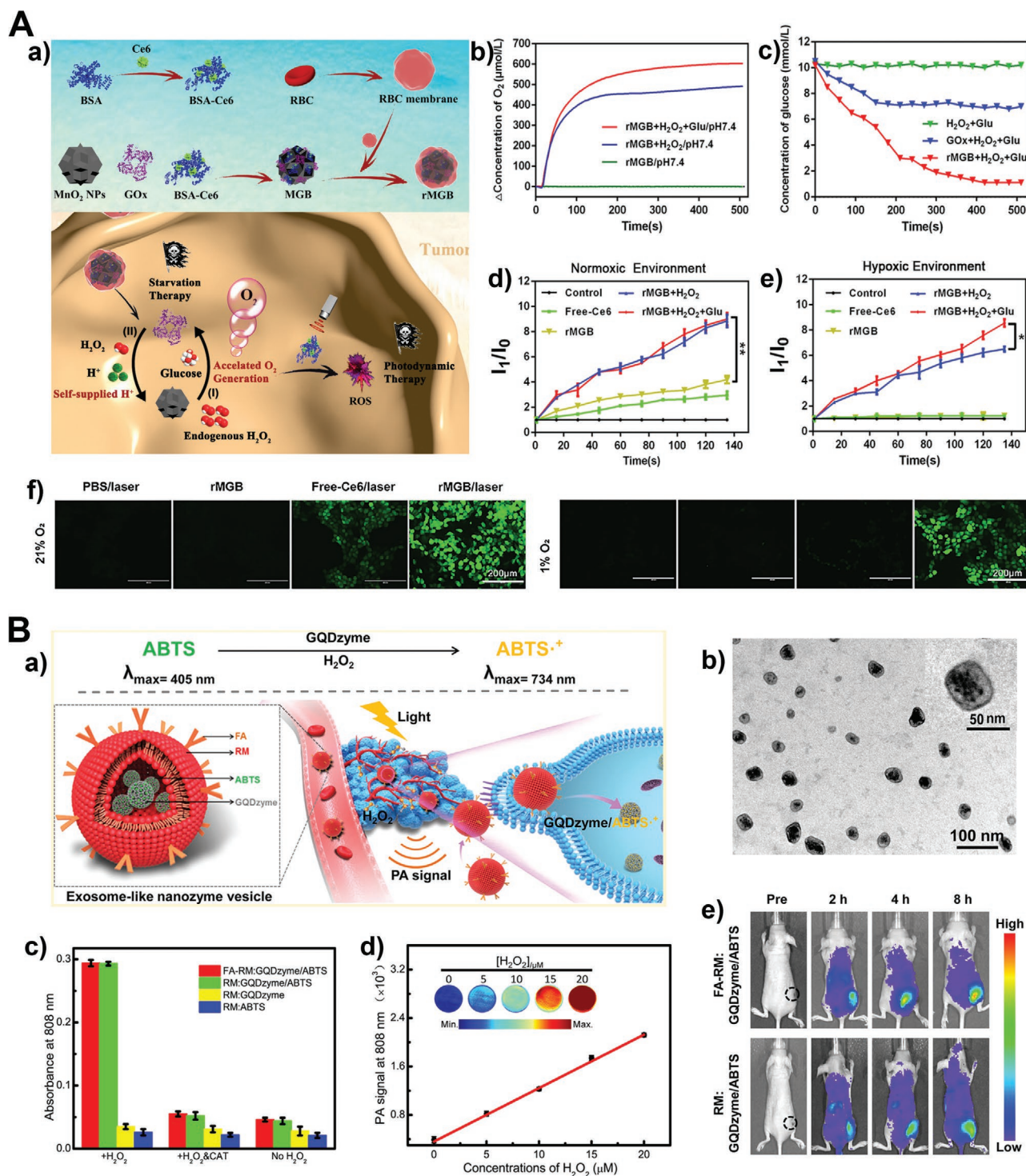


**Figure 9.** A-a) Preparation and mechanism illustration of the rMGB. b)  $O_2$  generation at pH = 7.4 in different samples. c) Glucose changes in different sample-mixed glucose solution. d)  $^1O_2$  generation after 660 nm irradiation in d) normoxic and e) hypoxic environment, and f) the detection of  $^1O_2$  in cells at these oxygen environments. (\* $p < 0.05$ , \*\* $p < 0.01$ ,  $n = 3$ , Scale bars represent 200  $\mu m$ .) Reproduced with permission.<sup>[205]</sup> Copyright 2019, American Chemical Society. B-a) Illustration of Exosome-like Enz-Ms vesicle and its antitumor mechanism. b) TEM image of RM: GQDzyme/ABTS. c) The absorbance of FA-RM: GQDzyme/ABTS at 808 nm in different solutions at 37 °C. d) Linear relationship analysis between FA-RM: GQDzyme/ABTS induced PA signal intensity and  $H_2O_2$  concentration. e) In vitro fluorescence images of xenograft tumor-bearing mice at 1, 3, and 6 h after intravenous injection of FA-RM: GQDzyme/ABTS. Reproduced with permission.<sup>[203]</sup> Copyright 2019, American Chemical Society.



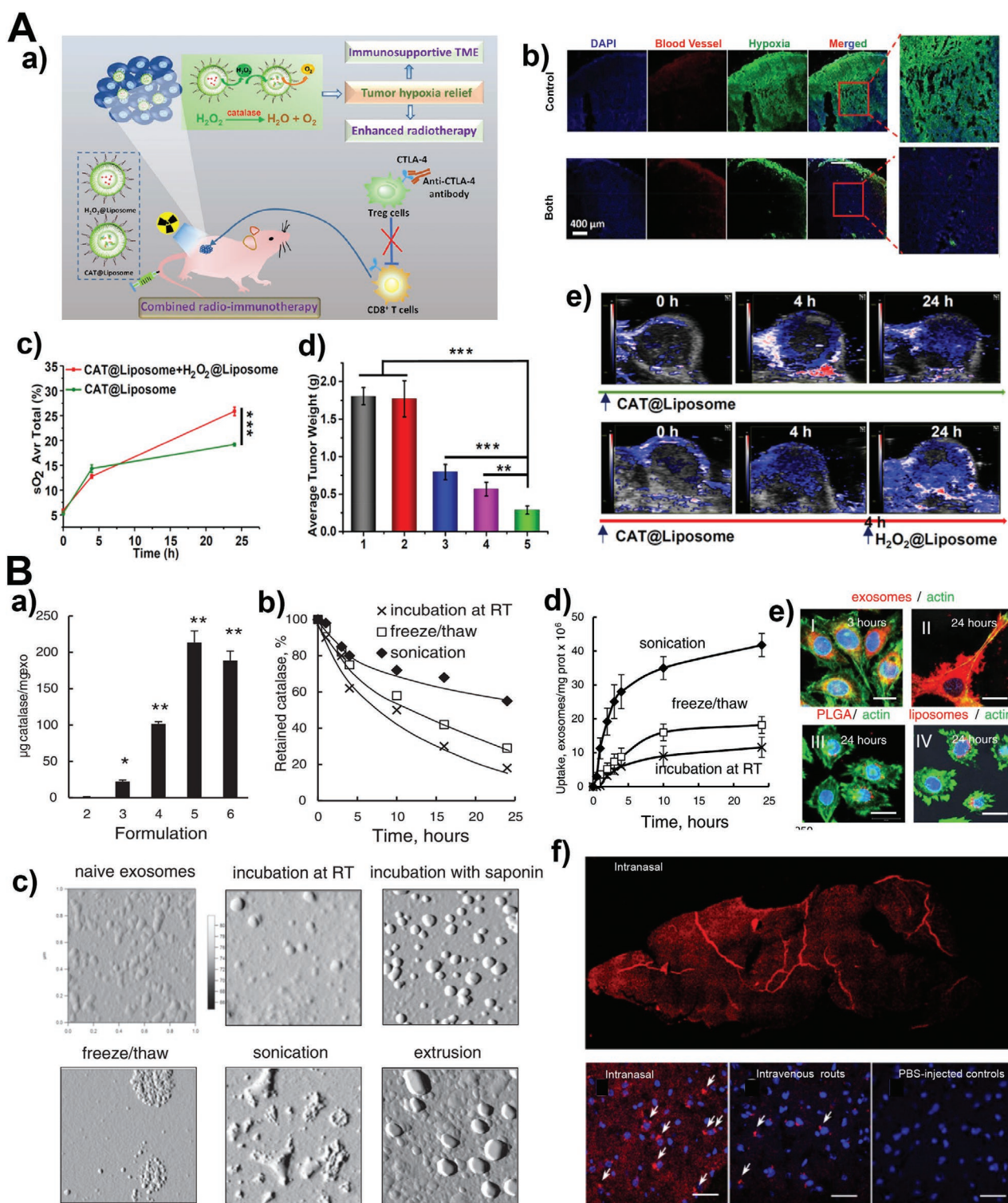


**Figure 10.** A-a) Tumor therapy illustration of CAT@liposome and H<sub>2</sub>O<sub>2</sub>@liposome. b) Tumor immunofluorescence images after different treatments, “both” represents the CAT@liposome and H<sub>2</sub>O<sub>2</sub>@liposome. c) Quantification of the oxyhemoglobin saturation in the total tumor area (sO<sub>2</sub> Avr Total) in (e). d) Average tumor weight at day 18 after different treatments including 1) control; 2) Both, X-ray −; 3) X-ray +; 4) CAT@Liposome, X-ray+; 5) Both, X-ray +. e) PA images of tumors after injected with CAT@Liposome or both liposomes. *p* values: \**p* < 0.05, \*\**p* < 0.01, \*\*\**p* < 0.001, ANOVA. Reproduced with permission.<sup>[217]</sup> Copyright 2018, American Chemical Society. B) Characterization of exoCAT. a) Catalase loading of different methods, including, 2—empty exosome; 3—incubation; 4—freeze/thaw; 5—sonication; 6—extrusion. b) CAT release efficiencies in different groups. c) AFM images of ExoCAT. d) The uptake efficiency of ExoCAT and e) their confocal microscopy images. Scale bar = 20 μm. f) The biodistribution of DIL-labeled exosomes in mouse brain. Scale bar = 40 μm. Reproduced with permission.<sup>[216]</sup> Copyright 2015, Elsevier Ltd.

exoCAT on the loading, release, and uptake of CAT, as well as their morphologies (Figure 10B-a-e). They also found that this exoCAT was widely distributed in the brain, proving the BBB across the abilities of exosomes and its cargo transportation ability (Figure 10B-f). Furthermore, the exoCAT injected PD mouse group significantly decreased microglial activation, indicating significant antiinflammatory and neuroprotective effects.

From the above section, we thoroughly discussed the different types of cell membranes and their analogs for Enz-Ms functionalization. Each type of the source cells owns specific biological properties, such as the inflammation homing of macrophages, prolonged blood circulation half-life time of RBC, when compared between these materials for their applicability in Enz-Ms delivery, it becomes evident that these source cells are somehow complementary since the most prominent features of each one do not always overlap. Therefore, researchers began to think about simultaneously coating different membrane components on nanomaterials and finally found that this idea is achievable. It was shown that the combination of RBC/platelets, RBC/tumor cells, as well as liposomes/exosomes, could be used in nanoparticles' camouflaging.<sup>[217–219]</sup> Therefore, the hybrid membrane can also be used to modify Enz-Ms, and the multifunctional hybrid complexes are expected to effectively treat diseases, such as tumors, neurodegenerative diseases, bacterial infections, and inflammation.

## 8. Surface-Decoration of Enz-Ms by Functional Polymers and Biopolymers

Synthetic polymers, such as polyethylene glycol (PEG),<sup>[220]</sup> polycaprolactones,<sup>[221]</sup> dextrans,<sup>[222]</sup> chitosan,<sup>[223]</sup> hyperbranched polyglycerol,<sup>[224,225]</sup> polyethyleneimine (PEI),<sup>[226]</sup> and amphiphilic lipid-PEG,<sup>[227]</sup> are typically organic polymers used in inorganic nanoparticles surface-modifications via “grafting to” method or “grafting from” method.<sup>[228–233]</sup> Besides, series of macromolecules (such as DNA,<sup>[234]</sup> proteins<sup>[235,236]</sup>) can also be anchored onto the surface of Enz-Ms via electrostatic adsorption, hydrophobic interaction, hydrogen bond formation, and molecular coordination. One could suppose that the regulation effects of macromolecular and the catalytic effects of Enz-Ms are interdependent. On the one hand, the modification of Enz-Ms by functional polymers or biopolymers can improve the biological properties, such as better biocompatibility, targeting effects, and prolonged blood circulation time.<sup>[232,237]</sup> On the other hand, the catalytic performances of Enz-Ms would be influenced by the thickness of the coating and the steric hindrance of macromolecules.<sup>[51]</sup>

### 8.1. Synthetic Polymers Decorated BF/Enz-Ms

One of the characteristics of surface modifications is that the surface coatings affect the size and catalytic performance of the Enz-Ms. For example, as shown in Figure 11A-a, Perez et al. found that a thinner and more permeable poly(acrylic acid)-coating of nanoceria showed a significant increase in catalytic activity and kinetics against TMB and ABTS than those with thicker coatings, which indicates that the polymer coating thickness is vital when oxidizing the substrate.<sup>[53]</sup> Meanwhile,

this kind of surface-modified nanoceria is expected to be a more robust and reliable TMB-based immunoassay than the traditional ELISA (horseradish peroxidase-based) as no extra enzyme or  $\text{H}_2\text{O}_2$  would be needed for detection (Figure 11A-b). Recently, Gao et al. found that the enzyme-mimetic activity of the polymers modified nanoparticles decreased compared to that of the bare nanoparticles since the catalytic activity of the Enz-Ms is closely related to its size. In contrast, the polymer modification usually causes a larger size and a blocking effect, whether with PEG or dextran modification.<sup>[34]</sup>

While the coating of the polymer can result in a partial reduction in catalytic activity, the polymer can also modulate the type of native enzyme-mimetic exhibited by the nanoparticles. Lin and co-workers reported that in physiological conditions, amine-terminated poly(amidoamine) dendrimer-entrapped gold nanoclusters ( $\text{AuNCs-NH}_2$ ) maintained the CAT-like activities but no longer peroxidase analogs,<sup>[54]</sup> and its CAT-like activity was not affected by different intracellular pH conditions (Figure 11B-b). When depleting  $\text{H}_2\text{O}_2$ , it showed significantly better results than  $\text{AuNCs-OH}$  attributed to larger hydrophilicity. It was also found that 3°-amines played leading roles in regulating the catalytic activity; therefore, as long as the main tertiary amines (3°-amines) of the dendrimer were blocked to form quaternary ammonium ions (4°-amines), the peroxidase activity of the methylated  $\text{AuNC-NH}_2$  can be significantly restored. This kind of characteristic shows an excellent possibility for protecting primary neuronal cells against oxidative stress-induced damage (Figure 11B-a,c).

It is known that different pH conditions influence the enzyme-like abilities of bare Enz-Ms; for instance, the iron oxide performs oxidase-mimics under neutral conditions and peroxidase-mimics under acidic conditions,<sup>[238]</sup> besides, gold nanoparticles only exhibit peroxidase activity under neutral conditions.<sup>[239]</sup> Therefore, it is necessary to regulate and stabilize enzyme-mimetic activity under a wide range of pH conditions. For example, Malinowska et al. found that Au nanoparticles stabilized with low molecular weight hyperbranched polyglycerol and its maleic acid residues derivative maintained peroxidase activity under a wide range of pH conditions, which may benefit from the effect that the charge of polymeric ligands on the activity of different types of substrates (anionic or cationic) is negligible.<sup>[240]</sup>

In addition to the regulation and stabilization of catalytic properties, polymer-modified Enz-Ms can also be applied in the anti-tumor and antibacterial applications.<sup>[241–244]</sup> For example, Zhao et al. prepared PEG-modified  $\text{MoS}_2$  nanoflowers (PEG- $\text{MoS}_2$  NFs), wherein the introduction of PEG imparted high biocompatibility and water solubility to the nanoparticles and prevented its aggregation in biofluids. Besides, due to the peroxidase-like and photothermal conversion activities of  $\text{MoS}_2$ , the system can achieve rapid and effective bacterial killing (including Gram-positive and Gram-negative bacteria) under the synergistic antibacterial effect of a large amount of  $\cdot\text{OH}$ , high temperature and accelerated the oxidation of glutathione caused by high temperature, thereby promoting wound healing.<sup>[47,245]</sup>

### 8.2. Biopolymers Decorated BF/Enz-Ms

Along with synthetic polymer modification, biopolymers modified nanoparticles also regulate their biological and catalytic

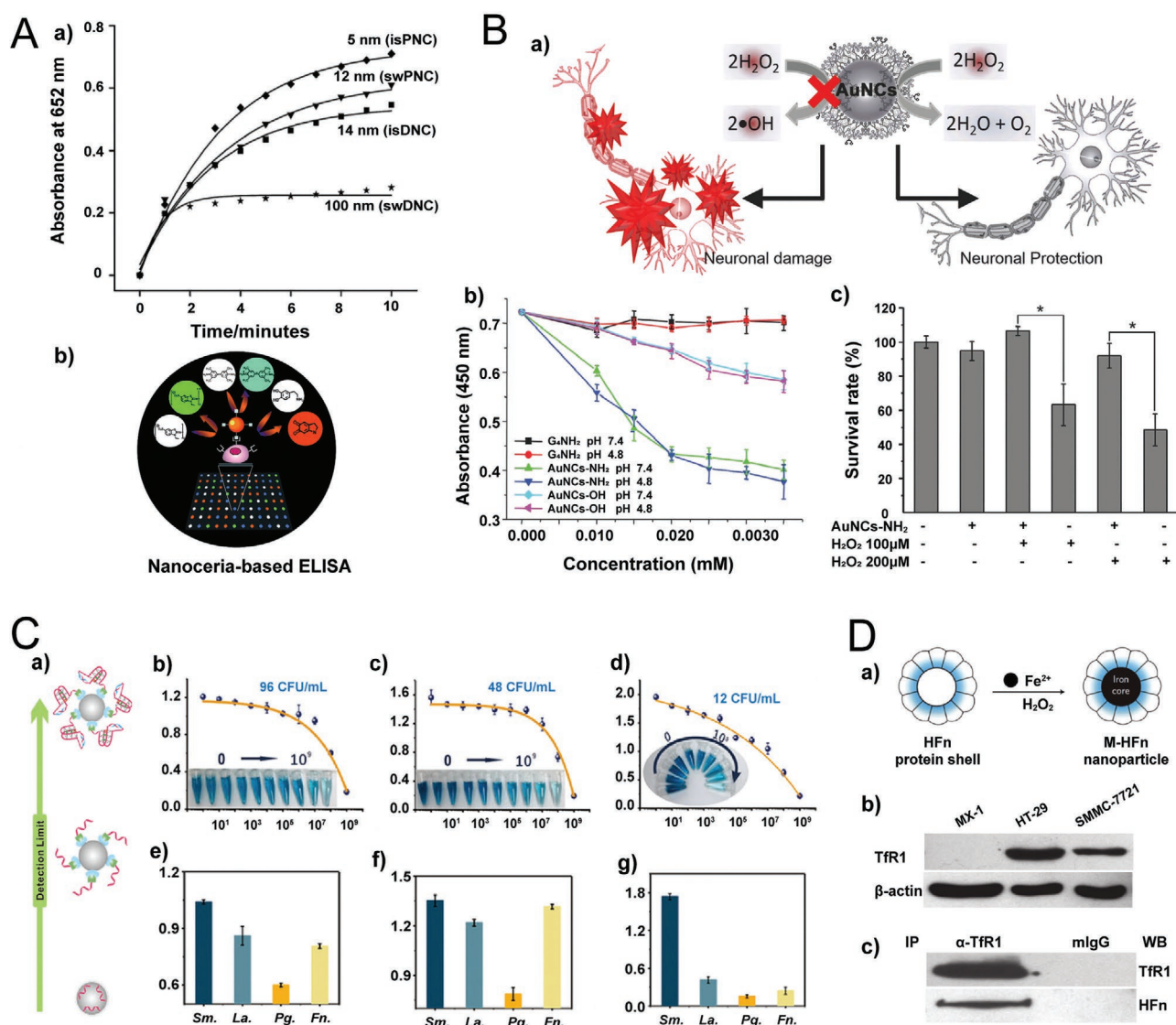


**Figure 11.** A-a) Size-dependent oxidation of TMB. Stepwise/in situ prepared DNC refers to swDNC/isDNC; in situ/stepwise prepared poly (acrylic acid) coated DNC refers to isPNC/ swPNC. b) Illustration of nanoceria-based ELISA. Reproduced with permission.<sup>[53]</sup> Copyright 2009, Wiley-VCH. B-a) Illustration of how dendrimer-encapsulated AuNCs protect neuronal against oxidative damage. b) Catalytic activities of  $G_4NH_2$ , AuNCs-OH, and AuNCs-NH<sub>2</sub> at pH of 4.8 and 7.4, respectively. c) Quantification of neurons survival rates. Reproduced with permission.<sup>[54]</sup> Copyright 2016, Wiley-VCH. C-a) Schematic illustration of the proposed colorimetric biosensors. b–d) Absorbance responses of *S. mutans* against three biosensors. e–g) The absorbance changes of *S. mutans*, *L. acidophilus*, *P. gingivalis*, *F. nucleatum* ( $10^9$  CFU mL<sup>-1</sup>) against three biosensors. Reproduced with permission.<sup>[249]</sup> Copyright 2019, American Chemical Society. D-a) A scheme of M-HFn nanoparticle. b) Western blot of TfR1 expression in HT-29, SMMC-7721, and MX-1 cells. c) Western blot of TfR1 immunoprecipitation by mouse anti-HFn mAbs and visualized with HRP-coupled antimouse IgG. Reproduced with permission.<sup>[250]</sup> Copyright 2012, Nature Publishing Group.

activities.<sup>[246]</sup> It has been reported that Au NPs modified with DNA have a GOx-like catalytic activity of 25–75% lower than that of unmodified ones;<sup>[247]</sup> however, some reports also showed that DNA-coating could improve the peroxidase activities of Au and Fe<sub>3</sub>O<sub>4</sub> nanoparticles attributed to an enhanced electrostatic attraction and aromatic stacking with the substrate TMB.<sup>[35,33,248]</sup> Except for the meditation of enzymatic performance, biopolymers modified Enz-Ms also have broad biological applications, for instance, in biosensors. Zhang et al. proposed a DNA-engineered Enz-Ms,<sup>[249]</sup> based on the use of DNA as a molecular recognition bond and adhesion substrates to functionalize Enz-Ms. Therefore,

it can rapidly, label-freely, and sensitively detect *Streptococcus mutans* by making the surface of Enz-Ms more approachable for bacteria via a colorimetric method, reaching a detection limit of 12 CFU mL<sup>-1</sup> (Figure 11C-a–d). Moreover, they also confirmed that it could identify dental bacteria in saliva samples, as well as excellent ability to distinguish from other dental bacteria (Figure 11C-e–g), thus indicating the clinical possibilities for prevention and diagnosis of dental diseases.

Furthermore, Yan and Liang's group synthesized magneto-ferritin-functionalized nanoparticles (M-HFn) as novel reagents for self-targeting and visualizing tumor tissue.<sup>[250]</sup> They used



recombinant human heavy-chain ferritin (HFn) to modify iron oxide nanoparticles to form nanocages (Figure 11D-a). Moreover, the HFn overexpressed transferrin receptor 1 protein has a very high affinity for tumor cells and thus can be actively targeted to tumor sites (Figure 11D-b-c). Besides, the peroxidase-like activity of iron oxide nanoparticles can catalyze the substrates and produce colored products for visualization of tumor tissue. By examining 474 clinical specimens (247 tumor tissue samples and 227 control samples) from 9 types of cancer, they confirmed that it could identify cancer cells from normal cells with a sensitivity of 98% and a specificity of 95%.<sup>[57]</sup>

### 8.3. Surface-Decorated BF/Enz-Ms as Biotherapeutic Agents

In the two sections above, we discussed the design of functional molecular-modified BF/Enz-Ms with different properties and their applications as biosensors and protectants. Likewise, using them as biotherapeutic agents is also an ideal choice. For example, Zhang et al. designed a nanosystem that actively targets tumors by coencapsulating GOD, MnO<sub>2</sub>, and glycoprotein CD44 targeted folate (Figure 12A-a,b).<sup>[251]</sup> The catalytic oxidation of glucose to H<sub>2</sub>O<sub>2</sub> through GOD, which also consumes O<sub>2</sub>, is concentration-dependent (Figure 12A-c). However, at the same time, MnO<sub>2</sub> can further react with H<sub>2</sub>O<sub>2</sub> to produce O<sub>2</sub> and alleviate the rapid consumption of glucose (Figure 12A-d), thus realizing the starvation therapy of tumors. Furthermore, the mass ratio of MnO<sub>2</sub> to GOD at O<sub>2</sub> equilibrium was determined to be 50:1 in a simulated tumor microenvironment (Figure 12A-e). At this ratio, although under hypoxia, the designed BF/Enz-Ms revealed excellent in vivo antitumor effects (Figure 12A-f).

In addition to the starvation treatment of tumors, the Enz-Ms with O<sub>2</sub> generation ability can also overcome the hypoxic environment in the deep part of tumors and enhance the PDT effects under NIR irradiation. Therefore, Zhu et al. designed a shell-core nanosheet, named as SPN-M1, by encapsulating MnO<sub>2</sub> with semiconductor polymer nanoparticles (SPN) (Figure 12B-a-c).<sup>[252]</sup> Figure 12B-d shows that the SPN-M1 can produce <sup>1</sup>O<sub>2</sub> through a series of transformations under the weak acidic condition of hypoxia, and its <sup>1</sup>O<sub>2</sub> production capacity is 3.8 times higher than that of SPN-0 without MnO<sub>2</sub> coating, while its photothermal effect is relatively weak (Figure 12B-e). In vivo antitumor experiments show that SPN-M1 in the PDT group has a significant inhibitory effect on tumor growth during the 15-day treatment (Figure 12B-f), making it possible for clinical application.

Overall, the introduction of synthetic polymers or biopolymers in the modification of Enz-Ms not only regulates the catalytic performance but also ensures the foundations for biological applications. Furthermore, multifunctional molecules may also be applied to modify Enz-Ms and provide better treatment efficiencies on bacterial disinfection/anticancer/antiinflammation.

## 9. Functional Molecules/Enz-Ms-Derived Nanocomposites

Nanocomposites generally refer to the addition of nanoparticles to a matrix material to improve the specific properties of the composites. Conventional nanocomposites are mostly based

on ceramic/metal/magnetic/polymer and can be used in the fields of electrochemistry, sensors, and biological therapy.<sup>[253]</sup> For functional molecules/Enz-Ms-derived nanocomposites, it provides unique chemical compositions and nanostructures for diverse advanced biological applications, for instance, the metal-organic complex-based hybridized BF/Enz-Ms exhibit easy fabrication and excellent bioactivity. Recently, Hao et al. reported a seed growth method for polymer shells coordinated by nucleotides using Fe<sup>3+</sup> as a metal-core and successfully formed a biofunctional shell (Figure 13A-a).<sup>[254]</sup> This polymer shell has a stable and high loading capacity for varieties of guest molecules, including proteins, DNA, and gold nanoparticles (Figure 13A-b,c). Besides, Fe-based peroxidase activity has been retained to serve as a glucose biosensor with a detection limit of  $1.4 \times 10^{-6}$  M (Figure 13A-d,e).

Due to the lack of sufficient methods, constructing multiple enzymatic centers on large proteins remains a long-standing problem to be solved. With the help of artificial enzyme mimics, like Enz-Ms, it is possible to achieve the multienzymatic centers on protein. For example, Liu's group reported constructing hybridized Enz-Ms by self-assembling the GPx on the protein monomers of the tobacco mosaic virus.<sup>[255]</sup> Since the GSH-dependent antioxidant activity of GPx enzyme, the constructed GPx-loaded Enz-Ms not only avoid the toxic and side effects caused by the conventional GPx simulated selenium-containing organic molecules but also has high recognition and catalytic abilities to eliminate ROS. These characteristics result in the protection of intracellular components against harmful processes such as the oxidative damage to mitochondria.

Based on the above research, the same group further utilized self-assembled cyclic protein SeSP1 and dendrimer polymeric nanoparticle MnPD5 with GPx and SOD activities, respectively, to construct the soft antioxidant composite nanowire (Figure 13B-a-c).<sup>[256]</sup> The TEM image confirmed the nanowire structure, making the alternate arrangements of the two enzymes visible (Figure 13B-d). The SP1-PG5 nanocomposites showed excellent enzymatic activity (Figure 13B-e), which can be used to clear over-expressed ROS in the body to avoid oxidative damage and hopefully to be applied in cardiovascular and neurodegenerative diseases.

As an essential component of Enz-Cat, the inorganic or metallic material was also assembled onto functional molecular matrices by physical or chemical methods, which can increase the bioavailability and improve the therapeutic effect of various diseases, such as cancer treatment and bacterial disinfection.<sup>[228,253]</sup> The proliferation of cancer cells requires their mitochondria to be much more active than healthy tissues. Hence, changes in the redox homeostasis of cancer cells result in high levels of ROS and antioxidants, such as glutathione (GSH).<sup>[257-259]</sup> By consuming GSH to break the balance of ROS and antioxidants, thus enabling the accumulation of abundant ROS in tumor tissues, thereby triggering apoptosis and killing cancer cells. For efficiently and rapidly consume GSH in mitochondria, Gong et al. proposed a feasible solution by supporting gold CAT-g with carbon dots to significantly improve the selectivity of the biochemical reaction between gold and GSH. Then, triphenylphosphine (TPP) and cinnamaldehyde (CA) are further modified on the surface to obtain MitoCAT-g (Figure 14a).<sup>[260]</sup> Upon reaching the mitochondria,

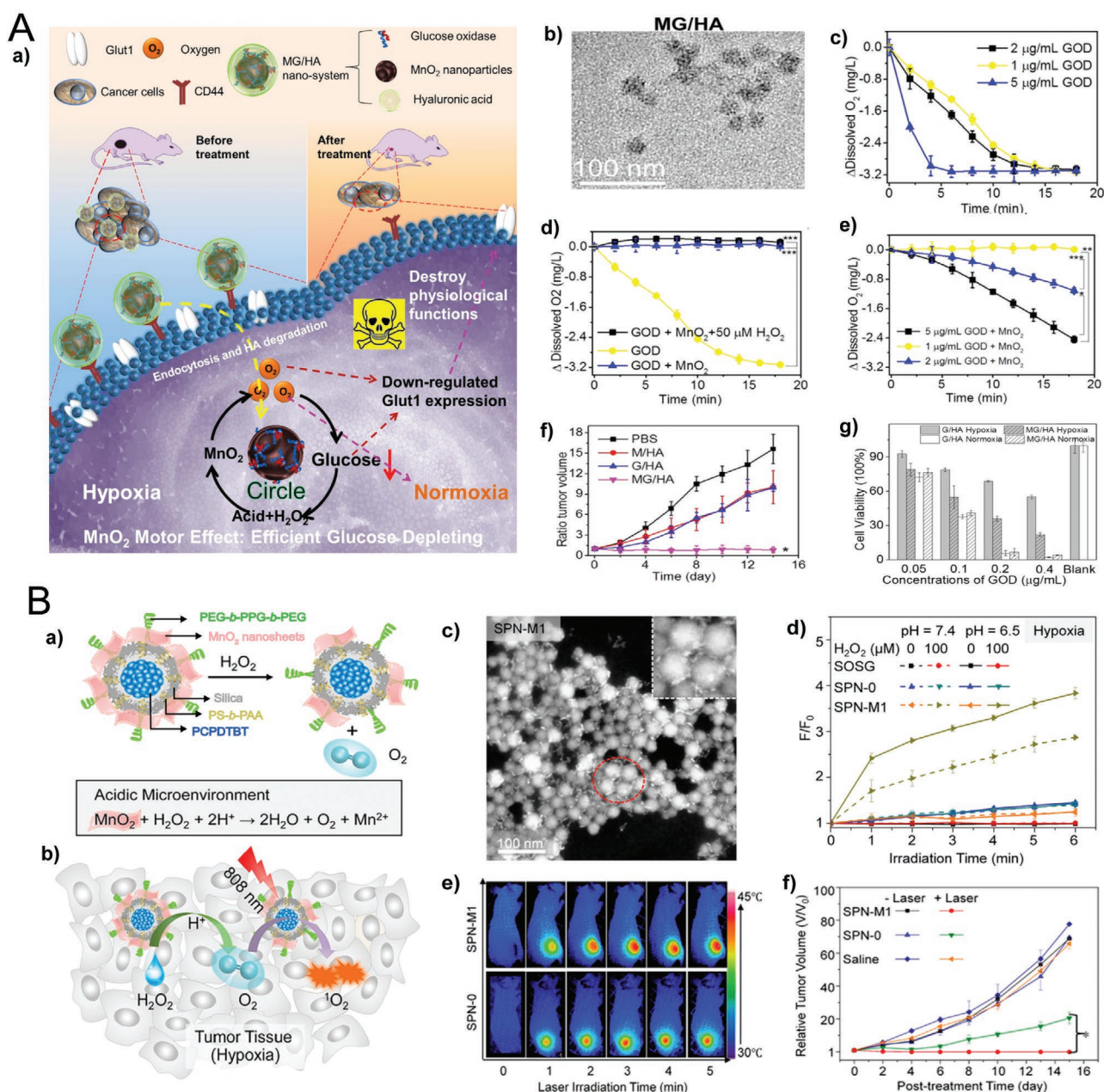


**Figure 12.** A-a) Illustration of the MnO<sub>2</sub> nanocatalytic effects in the MG/HA system for antitumor therapy. b) TEM image of MG/HA nanocatalysts. c) The  $\Delta$ -dissolved O<sub>2</sub> mediated by glucose and GOD.  $\Delta$ -dissolved O<sub>2</sub> mediated by MnO<sub>2</sub> and GOD in d) glucose solutions and e) mimic microenvironment solutions. f) Tumor volume changes in 16 days of different samples. g) Cell viabilities of G/HA and MG/HA cultured in hypoxia and normoxia. Reproduced with permission.<sup>[251]</sup> Copyright 2018, American Chemical Society. B-a) Illustration for the H<sub>2</sub>O<sub>2</sub>-responsive and antitumor mechanisms of SPN-M1. b) STEM image of SPN-M1. c) Detection of <sup>1</sup>O<sub>2</sub> by SOSG for SPN-0 or SPN-M1 with or without H<sub>2</sub>O<sub>2</sub> under hypoxic conditions at 808 nm NIR light (0.44 W cm<sup>-2</sup>). [SPN] = 10  $\mu$ g mL<sup>-1</sup> in 1  $\times$  PBS (pH 7.4). c) Infrared thermal images of tumor-bearing mice at 808 nm NIR light (0.3 W cm<sup>-2</sup>). d) Tumor volume changes in 16 days of SPN-0, SPN-M1, and saline with or without NIR irradiation. Reproduced with permission.<sup>[252]</sup> Copyright 2018, American Chemical Society.

CA is released due to the weak acid environment, which then directs the production of ROS; meanwhile, the TPP-CAT-g particles capture GSH to form gold-sulfur bonds and deplete the antioxidant GSH, thus amplifying oxidative stress and promoting cell apoptosis (Figure 14c,b). After 43 days of treatment by using a xenograft model of HCC tumor (Figure 14d), the MitoCAT-g group shows significant tumor suppression (Figure 14e), and the survival rate of mice treated by MitoCAT-g

remains 75% at 93 days, while the other groups all died within 60 days (Figure 14f). Overall, we believe that the functional molecule/metal nanocomposites-derived BF/Enz-Ms also play an indispensable role in future treatments. Therefore, innovative structures and new synthetic methods should be carefully investigated to improve their enzyme-mimetic catalytic performance further and expand their bioactivity by the integration of various bioactive inorganic or metallic components.



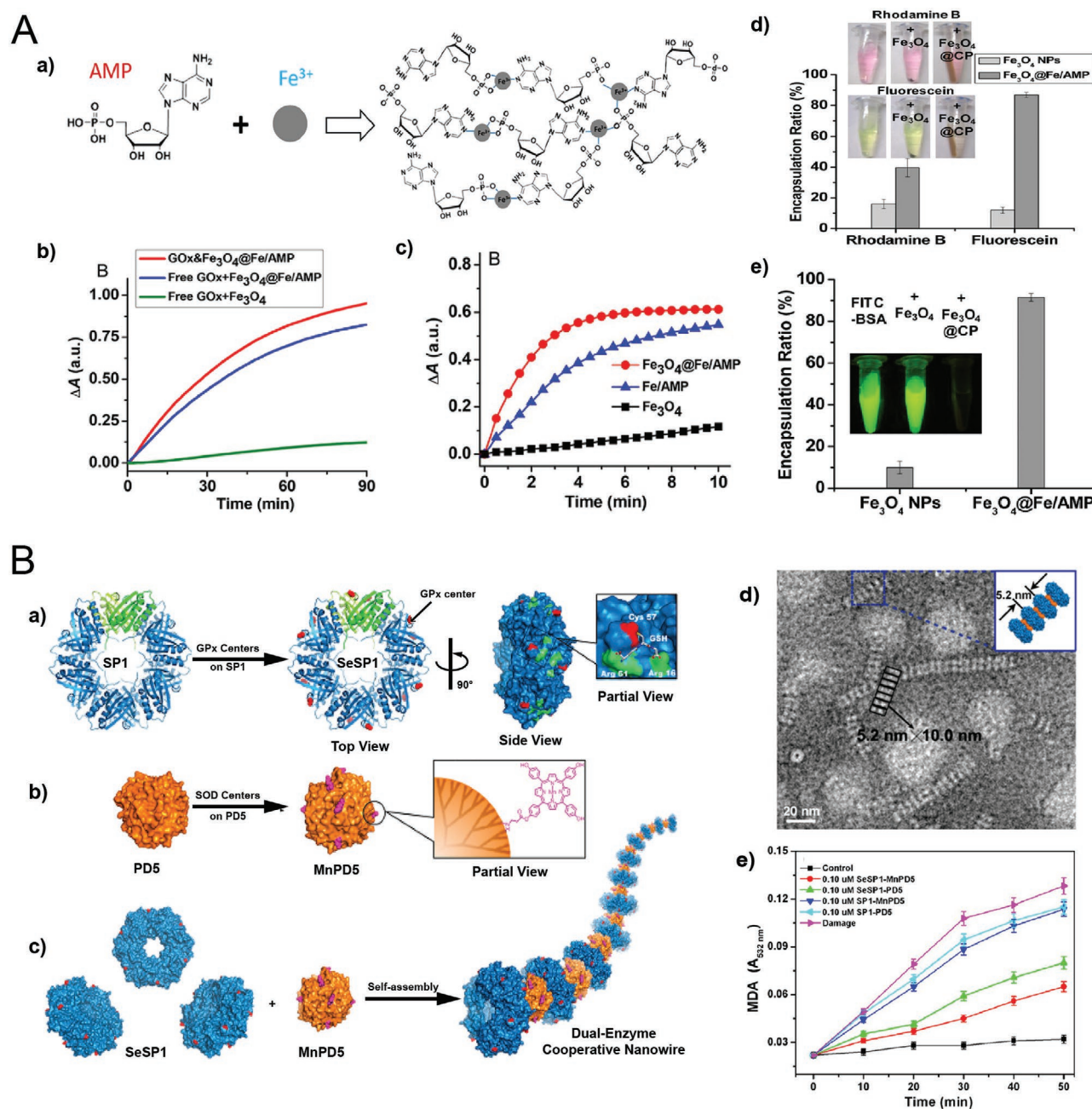


**Figure 13.** A-a) Schematic image of the formation of polymer shells. Encapsulation ratio of b) fluorescein and rhodamine B, c) BSA-mixed Fe<sub>3</sub>O<sub>4</sub> NPs or Fe<sup>3+</sup>/AMP CP. Oxidation kinetics of ABTS in different groups in the presence of d) H<sub>2</sub>O<sub>2</sub> and e) GOx. Reproduced with permission.<sup>[254]</sup> Copyright 2016, American Chemical Society. B) Illustration of the construction of a) SeSP1, b) MnPD5, and c) dual-enzyme cooperative nanowire. d) TEM image of the dual-enzyme cooperative nanowire. e) Scavenging abilities of superoxide anion radicals of different groups. Reproduced with permission.<sup>[256]</sup> Copyright 2015, American Chemical Society.

## 10. Conclusions and Perspectives

In recent years, significant breakthroughs have been made in the use of Enz-Ms to mimic the catalytic activity of natural enzymes.<sup>[58,59]</sup> In this progress report, we discuss the influence of functional molecules and nanostructures on the catalytic and biological performances of diverse BF/Enz-Ms and summarize the structure-function relationship in diverse biomedical

applications of BF/Enz-Ms, including biosensing, tumor therapy, and treatment of bacterial infections.

Though, it is difficult to conclude which BF/Enz-Ms is the best candidate for future biomedical applications. In general, for drugs/proteins/enzymes delivery and regenerative therapeutics, the hydrogels and microgels engineered BF/Enz-Ms hold the promising potential due to their 3D structures, high biocompatibility, and ability to protect unstable NPs from fast



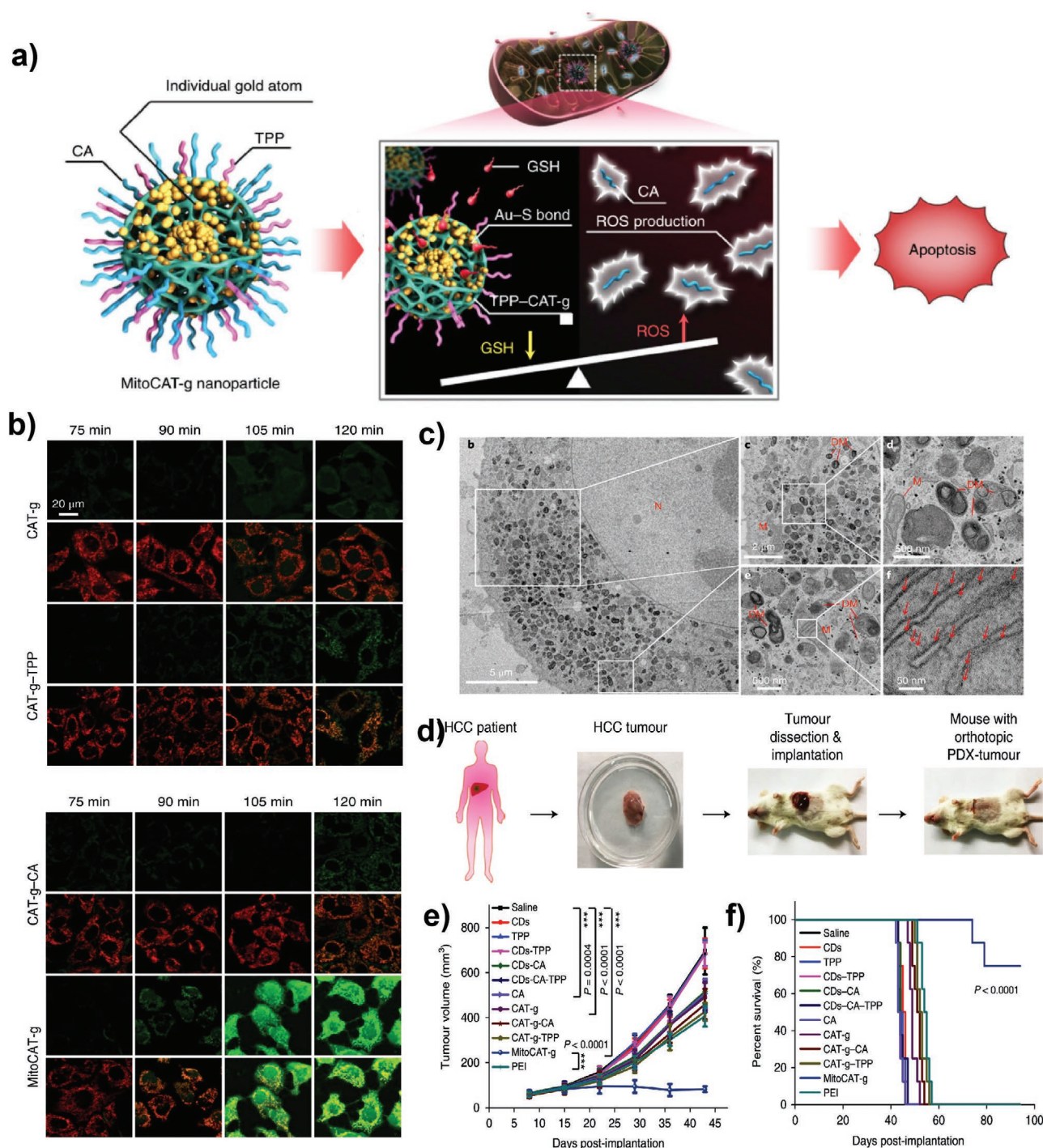


**Figure 14.** a) Illustration of the structure and antitumor mechanism of MitoCAT-g. b) CLSM images of HepG-2 cells with different groups after 75, 90, 105, and 120 min treatment. c) Bio-TEM image of MitoCAT-g-encapsulated HepG-2 cells. d) Illustration of the human HCC xenograft tumor model in mice. e) Tumor volumes changes measured by ultrasound imaging in 43 days. f) Kaplan–Meier survival curves of mice in various treated groups. Reproduced with permission.<sup>[260]</sup> Copyright 2019, Nature Publishing Group.

degradation. While, when designing nanomedicines with precise molecular/atomic-level biocatalytic centers and high porosity for drug loading, the functionalized MOFs and MPNs are supposed to be the most qualified BF/Enz-Ms for further

exploration in clinical applications. As for homotypic targeting and immunomodulation, the cell membranes decorated BF/Enz-Ms also present enormous application potential, which can endow the traditional Enz-Ms with self-targeted deliveries,

extended half-life of blood circulation, and many other biological properties, making the engineered BF/Enz-Ms more intelligent and stealth to the immune system.

Although the biomedical applications of BF/Enz-Ms as biocatalytic medicines or diagnostic agents are still in their infancy, they have shown promising application prospects due to its excellent catalytic performances and therapeutic effects. It is imperative to combine these introduced chemical protocols, engineering technics, or rational design of intelligent moieties to construct the BF/Enz-Ms system to achieve targeted delivery, controllable releasing, and more efficient catalytic therapeutics and diagnostics. Nevertheless, some foreseeable challenges and critical issues to expand its further application scope needs to be paid attention to and given solve strategies.<sup>[45,145]</sup>

- 1) Many of the Enz-Ms have revealed similar catalytic capabilities as that of natural enzymes.<sup>[34,35]</sup> However, integrating the excellent functionalities and biocompatibility of functional molecules BF/Enz-Ms may significantly affect their catalytic performances. Although some studies references have reported that BF/Enz-Ms have better enzymatic activity, in general, their enzymatic activities are reduced after functionalization. Therefore, how to balance the catalytic activities and the surface functionalization modifications are worth further consideration. A typical example is the PEG coating on the surface of nanoparticles, such as Fe<sub>3</sub>O<sub>4</sub>,<sup>[34]</sup> with PEG introduced to prolong the circulation time and reach the lesion site. However, the presence of polymer coating and the thickness of the coating affect the catalytic performance of BF/Enz-Ms.<sup>[35,230,261]</sup>
- 2) Usually, the application of BF/Enz-Ms mainly focused on biosensing, cancer therapy, bacterial eradication, and cell protection against oxidative stress, and a few studies have highlighted the alleviation or treatment of Alzheimer's disease, Parkinson's disease, diabetes, and arthritis.<sup>[16,166,183,221,262,263]</sup> To maximize the synergistic effect for multimodal transmission or treatment and broaden the biomedical applications of BF/Enz-Ms, many new types of nanostructures, energy conversion therapies, and functional therapeutic drugs can be integrated,<sup>[264,265]</sup> or through the construction of hybrid membrane carriers, such as platelets/cancer cells and liposomes/exosomes.<sup>[214,264,266]</sup>
- 3) Although BF/Enz-Ms exhibit excellent potential for antimicrobial, antitumor, and alleviating neurodegenerative diseases, their catalytic mechanisms in vivo remain unclear. Appropriate model and theoretical calculations are of great significance for identifying reaction intermediates and understanding the possible catalytic kinetics and mechanism of BF/Enz-Ms in biomedicine.
- 4) Intelligent systems of BF/Enz-Ms usually have complex structures and multiple components to realize the simulation of specific or multiple enzymes, and their preparation methods are often complicated and not suitable for large-scale production. Moreover, the biocatalytic performance and morphological structure of BF/Enz-Ms may be different between different synthetic batches, and how to standardize, normalize, and produce BF/Enz-Ms on a large scale are also urgent problems that remain unsolved.

- 5) To translate BF/Enz-Ms as nanomedicines or diagnostic agents into clinical practice for diverse diseases, the in vivo metabolism of Enz-Ms also needs to be considered in detail. Adverse reactions due to the potential long-term toxicity of biocatalytic inorganic/metallic particles in BF/Enz-Ms to healthy tissues will hinder the potential application in the biomedical area. Therefore, by establishing appropriate pharmacokinetic models, further studies on the metabolic pathways and in vivo deposition of BF/Enz-Ms can provide a deeper understanding of their in vivo action process, thus accurately constructing biocompatible BF/Enz-Ms, making a significant impact on future clinical applications.

As a summary of recent studies on emerging BF/Enz-Ms, all we can describe is just their initial state on the developments and applications in biomedical areas. We also believe that with the increased understanding of the design and synthesis of BF/Enz-Ms, highly efficient and intelligent BF/Enz-Ms systems will drive future progress in diverse biomedical and clinical applications.

## Acknowledgements

Q.T. and S.J.C. contributed equally to this work. This work was financially supported by the National Key R&D Program of China (2019YFA0110600 and 2019YFA0110601), National Natural Science Foundation of China (Nos. 82071938, 82001824, 51903178, 81971622, 51803134, and 51703141), the Science and Technology Project of Sichuan Province (Nos. 18YYJC1417, 2019YFS0219, 2020YFH0087, and 2020YJ0055), Special Funds for Prevention and Control of COVID-19 of Sichuan University (2020scunCoV-YJ-20005) and SKLFPM, Donghua University (YJ202005), and the Post-Doctor Research Project, West China Hospital, Sichuan University (No. 2018HXBH077). Prof. Cheng acknowledges the support of the State Key Laboratory of Polymer Materials Engineering (No. sklpme2019-2-03), Fundamental Research Funds for the Central Universities, Thousand Youth Talents Plan, and Alexander von Humboldt Fellowship. The authors thank our laboratory members for their generous help and gratefully acknowledge the help of Ms. Xijing Yang and Ms. Zhen Yang of the Animal Experimental Center, West China Hospital, as well as Dr. Chao He and Dr. Mi Zhou at Sichuan University.

## Conflict of Interest

The authors declare no conflict of interest.

## Keywords

antioxidation, biocatalytic nanomaterials, biofunctional polymers, biomedical applications, enzyme mimics

Received: September 1, 2020

Revised: October 15, 2020

Published online: November 2, 2020

[1] P. Bertrand, in *Electron Paramagnetic Resonance Spectroscopy*, Springer, Berlin 2020, p. 137.

[2] K. Chen, F. H. Arnold, *Nat. Catal.* 2020, 3, 203.

[3] B. P. Kumar, A. J. Patil, S. Mann, *Nat. Chem.* 2018, 10, 1154.

- [4] M. Wen, J. Ouyang, C. Wei, H. Li, W. Chen, Y. N. Liu, *Angew. Chem., Int. Ed.* **2019**, 58, 17425.
- [5] Y. Li, G. Liu, X. Wang, J. Hu, S. Liu, *Angew. Chem., Int. Ed.* **2016**, 55, 1760.
- [6] Z. Li, Y. Ding, S. Li, Y. Jiang, Z. Liu, J. Ge, *Nanoscale* **2016**, 8, 17440.
- [7] Q. Wu, Z. He, X. Wang, Q. Zhang, Q. Wei, S. Ma, C. Ma, J. Li, Q. Wang, *Nat. Commun.* **2019**, 10, 240.
- [8] S. Singh, *Nanosci. Technol.* **2017**, 5, 1.
- [9] T. Wang, X. Fan, C. Hou, J. Liu, *Curr. Opin. Struct. Biol.* **2018**, 51, 19.
- [10] Z. Chen, C. Zhao, E. Ju, H. Ji, J. Ren, B. P. Binks, X. Qu, *Adv. Mater.* **2016**, 28, 1682.
- [11] Z. Ma, L. Wu, K. Han, H. Han, *Nanoscale Horiz.* **2019**, 4, 1124.
- [12] J. Chen, W. Wu, L. Huang, Q. Ma, S. Dong, *Chem. - Eur. J.* **2019**, 25, 11940.
- [13] Y. Cheng, Y. Chang, Y. Feng, H. Jian, Z. Tang, H. Zhang, *Angew. Chem., Int. Ed.* **2018**, 57, 246.
- [14] D. Xu, X. Liu, H. Lv, Y. Liu, S. Zhao, M. Han, J. Bao, J. He, B. Liu, *Chem. Sci.* **2018**, 9, 4451.
- [15] Z. Chang, Y. Yang, J. He, J. F. Rusling, *Dalton Trans.* **2018**, 47, 14139.
- [16] F. Cao, L. Zhang, H. Wang, Y. You, Y. Wang, N. Gao, J. Ren, X. Qu, *Angew. Chem., Int. Ed.* **2019**, 58, 16236.
- [17] Y. Huang, C. Liu, F. Pu, Z. Liu, J. Ren, X. Qu, *Chem. Commun.* **2017**, 53, 3082.
- [18] J. Wang, L. Fang, P. Li, L. Ma, W. Na, C. Cheng, Y. Gu, D. Deng, *Nano-Micro Lett.* **2019**, 11, 74.
- [19] T. Zhang, Y. Song, Y. Xing, Y. Gu, X. Yan, H. Liu, N. Lu, H. Xu, Z. Xu, Z. Zhang, *Nanoscale* **2019**, 11, 20221.
- [20] L. Wang, Y. Chen, *ACS Appl. Mater. Interfaces* **2020**, 12, 8351.
- [21] K. Herget, H. Frerichs, F. Pfützner, M. N. Tahir, W. Tremel, *Adv. Mater.* **2018**, 30, 1707073.
- [22] M. Liang, X. Yan, *Acc. Chem. Res.* **2019**, 52, 2190.
- [23] Y. Hu, H. Cheng, X. Zhao, J. Wu, F. Muhammad, S. Lin, J. He, L. Zhou, C. Zhang, Y. Deng, P. Wang, Z. Zhou, S. Nie, H. Wei, *ACS Nano* **2017**, 11, 5558.
- [24] X. Xia, J. Zhang, N. Lu, M. J. Kim, K. Ghale, Y. Xu, E. McKenzie, J. Liu, H. Ye, *ACS Nano* **2015**, 9, 9994.
- [25] S.-Y. Li, H. Cheng, B.-R. Xie, W.-X. Qiu, J.-Y. Zeng, C.-X. Li, S.-S. Wan, L. Zhang, W.-L. Liu, X.-Z. Zhang, *ACS Nano* **2017**, 11, 7006.
- [26] X. Wang, L. Qin, M. Zhou, Z. Lou, H. Wei, *Anal. Chem.* **2018**, 90, 11696.
- [27] Y. Hao, Y. Liu, Y. Wu, N. Tao, D. Lou, J. Li, X. Sun, Y.-N. Liu, *Biomater. Sci.* **2020**, 8, 1830.
- [28] M. Hu, K. Korschelt, P. Daniel, K. Landfester, W. Tremel, M. B. Bannwarth, *ACS Appl. Mater. Interfaces* **2017**, 9, 38024.
- [29] C. X. Nie, L. Ma, S. Li, X. Fan, Y. Yang, C. Cheng, W. F. Zhao, C. S. Zhao, *Nano Today* **2019**, 26, 57.
- [30] W. Shao, C. He, M. Zhou, C. Yang, Y. Gao, S. Li, L. Ma, L. Qiu, C. Cheng, C. Zhao, *J. Mater. Chem. A* **2020**, 8, 3168.
- [31] C. Yang, M. Zhou, C. He, Y. Gao, S. Li, X. Fan, Y. Lin, F. Cheng, P. Zhu, C. Cheng, *Nano-Micro Lett.* **2019**, 11, 87.
- [32] J. Hu, P. Ni, H. Dai, Y. Sun, Y. Wang, S. Jiang, Z. Li, *Analyst* **2015**, 140, 3581.
- [33] M. S. Hizir, M. Top, M. Balcioglu, M. Rana, N. M. Robertson, F. Shen, J. Sheng, M. V. Yigit, *Anal. Chem.* **2016**, 88, 600.
- [34] L. Gao, J. Zhuang, L. Nie, J. Zhang, Y. Zhang, N. Gu, T. Wang, J. Feng, D. Yang, S. Perrett, *Nat. Nanotechnol.* **2007**, 2, 577.
- [35] B. Liu, J. Liu, *Nano Res.* **2017**, 10, 1125.
- [36] F. Gong, L. Cheng, N. Yang, Q. Jin, L. Tian, M. Wang, Y. Li, Z. Liu, *Nano Lett.* **2018**, 18, 6037.
- [37] H. Zhu, Y. Fang, Q. Miao, X. Qi, D. Ding, P. Chen, K. Pu, *ACS Nano* **2017**, 11, 8998.
- [38] S. Grundner, M. A. C. Markovits, G. Li, M. Tromp, E. A. Pidko, E. J. M. Hensen, A. Jentys, M. Sanchez-Sanchez, J. A. Lercher, *Nat. Commun.* **2015**, 6, 7546.
- [39] W. Jiang, Z. Zhang, Q. Wang, J. Dou, Y. Zhao, Y. Ma, H. Liu, H. Xu, Y. Wang, *Nano Lett.* **2019**, 19, 4060.
- [40] P. Zhu, Y. Chen, J. Shi, *ACS Nano* **2018**, 12, 3780.
- [41] C. Zhang, K. Zhao, W. Bu, D. Ni, Y. Liu, J. Feng, J. Shi, *Angew. Chem., Int. Ed.* **2015**, 54, 1770.
- [42] Z. Cheng, Y. Cheng, Q. Chen, M. Li, J. Wang, H. Liu, M. Li, Y. Ning, Z. Yu, Y. Wang, H. Wang, *Nano Today* **2020**, 33, 100878.
- [43] Q. Chang, H. Tang, *Microchim. Acta* **2014**, 181, 527.
- [44] X. Chen, B. Su, Z. Cai, X. Chen, M. Oyama, *Sens. Actuators, B* **2014**, 201, 286.
- [45] H. Xiang, W. Feng, Y. Chen, *Adv. Mater.* **2020**, 32, 1905994.
- [46] C. Cheng, S. Li, A. Thomas, N. A. Kotov, R. Haag, *Chem. Rev.* **2017**, 117, 1826.
- [47] Y. Huang, J. Ren, X. Qu, *Chem. Rev.* **2019**, 119, 4357.
- [48] B. Yang, Y. Chen, J. Shi, *Chem. Rev.* **2019**, 119, 4881.
- [49] S. Li, C. Cheng, X. J. Zhao, J. Schmidt, A. Thomas, *Angew. Chem., Int. Ed.* **2018**, 57, 1856.
- [50] C. Cheng, S. Li, Y. Xia, L. Ma, C. Nie, C. Roth, A. Thomas, R. Haag, *Adv. Mater.* **2018**, 30, 1802669.
- [51] H. Dong, Y. Fan, W. Zhang, N. Gu, Y. Zhang, *Bioconjug. Chem.* **2019**, 30, 1273.
- [52] J. Wu, X. Wang, Q. Wang, Z. Lou, S. Li, Y. Zhu, L. Qin, H. Wei, *Chem. Soc. Rev.* **2019**, 48, 1004.
- [53] A. Asati, S. Santra, C. Kaittanis, S. Nath, J. M. Perez, *Angew. Chem., Int. Ed.* **2009**, 48, 2308.
- [54] C. P. Liu, T. H. Wu, Y. L. Lin, C. Y. Liu, S. Wang, S. Y. Lin, *Small* **2016**, 12, 4127.
- [55] N. L. Klyachko, R. Polak, M. J. Haney, Y. Zhao, R. J. Gomes Neto, M. C. Hill, A. V. Kabanov, R. E. Cohen, M. F. Rubner, E. V. Batrakova, *Biomaterials* **2017**, 140, 79.
- [56] B. Du, X. Yan, X. Ding, Q. Wang, Q. Du, T. Xu, G. Shen, H. Yao, J. Zhou, *ACS Biomater. Sci. Eng.* **2018**, 4, 4132.
- [57] H. Wei, E. Wang, *Chem. Soc. Rev.* **2013**, 42, 6060.
- [58] D. Jiang, D. Ni, Z. T. Rosenkrans, P. Huang, X. Yan, W. Cai, *Chem. Soc. Rev.* **2019**, 48, 3683.
- [59] H. Wang, K. Wan, X. Shi, *Adv. Mater.* **2019**, 31, 1805368.
- [60] M. Li, H. Zhang, Y. Hou, X. Wang, C. Xue, W. Li, K. Cai, Y. Zhao, Z. Luo, *Nanoscale Horiz.* **2020**, 5, 202.
- [61] Y. Wang, R. Cai, C. Chen, *Acc. Chem. Res.* **2019**, 52, 1507.
- [62] F. Li, W. Ma, J. Liu, X. Wu, Y. Wang, J. He, *Anal. Bioanal. Chem.* **2018**, 410, 543.
- [63] Y. Song, K. Qu, C. Zhao, J. Ren, X. Qu, *Adv. Mater.* **2010**, 22, 2206.
- [64] P. Zhang, D. Sun, A. Cho, S. Weon, S. Lee, J. Lee, J. W. Han, D.-P. Kim, W. Choi, *Nat. Commun.* **2019**, 10, 1.
- [65] R. Godin, Y. Wang, M. A. Zwiijnenburg, J. Tang, J. R. Durrant, *J. Am. Chem. Soc.* **2017**, 139, 5216.
- [66] S. S. Ali, J. I. Hardt, K. L. Quick, J. S. Kim-Han, B. F. Erlanger, T.-t. Huang, C. J. Epstein, L. L. Dugan, *Free Radical Biol. Med.* **2004**, 37, 1191.
- [67] D. Nozdrenko, D. Zavodovskiy, T. Y. Matvienko, S. Y. Zay, K. Bogutska, Y. I. Prylutsky, U. Ritter, P. Scharff, *Nanoscale Res. Lett.* **2017**, 12, 115.
- [68] B. Xu, H. Wang, W. Wang, L. Gao, S. Li, X. Pan, H. Wang, H. Yang, X. Meng, Q. Wu, L. Zheng, S. Chen, X. Shi, K. Fan, X. Yan, H. Liu, *J. Am. Chem. Soc.* **2019**, 58, 4911.
- [69] C. Wang, D. Wang, S. Liu, P. Jiang, Z. Lin, P. Xu, K. Yang, J. Lu, H. Tong, L. Hu, W. Zhang, Q. Chen, *J. Catal.* **2020**, 389, 150.
- [70] Q. Chen, M. Liu, J. Zhao, X. Peng, X. Chen, N. Mi, B. Yin, H. Li, Y. Zhang, S. Yao, *Chem. Commun.* **2014**, 50, 6771.
- [71] S. N. Petrache, L. Stanca, A. I. Serban, C. Sima, A. C. Staicu, M. C. Munteanu, M. Costache, R. Burlacu, O. Zarnescu, A. Dinischiotu, *Int. J. Mol. Sci.* **2012**, 13, 10193.
- [72] S. Ansar, S. M. Alshehri, M. Abudawood, S. S. Hamed, T. Ahamad, *Int. J. Nanomed.* **2017**, 12, 7789.



- [73] Y. Huang, Z. Liu, C. Liu, Y. Zhang, J. Ren, X. Qu, *Chem. - Eur. J.* **2018**, *24*, 10224.
- [74] Z. Jin, G. Xu, Y. Niu, X. Ding, Y. Han, W. Kong, Y. Fang, H. Niu, Y. Xu, *J. Mater. Chem. B* **2020**, *8*, 3513.
- [75] K. Rasool, M. Helal, A. Ali, C. E. Ren, Y. Gogotsi, K. A. Mahmoud, *ACS Nano* **2016**, *10*, 3674.
- [76] Q. Gao, X. Zhang, W. Yin, D. Ma, C. Xie, L. Zheng, X. Dong, L. Mei, J. Yu, C. Wang, *Small* **2018**, *14*, 1802290.
- [77] H. Wang, S. Jiang, W. Shao, X. Zhang, S. Chen, X. Sun, Q. Zhang, Y. Luo, Y. Xie, *J. Am. Chem. Soc.* **2018**, *140*, 3474.
- [78] S.-Y. Cho, H.-J. Koh, H.-W. Yoo, H.-T. Jung, *Chem. Mater.* **2017**, *29*, 7197.
- [79] J. Shao, H. Xie, H. Huang, Z. Li, Z. Sun, Y. Xu, Q. Xiao, X.-F. Yu, Y. Zhao, H. Zhang, H. Wang, P. K. Chu, *Nat. Commun.* **2016**, *7*, 12967.
- [80] L. Chan, P. Gao, W. Zhou, C. Mei, Y. Huang, X.-F. Yu, P. K. Chu, T. Chen, *ACS Nano* **2018**, *12*, 12401.
- [81] L. Gao, X. Yan, *Adv. Exp. Med. Biol.* **2019**, *1174*, 291.
- [82] L. Gao, K. Fan, X. Yan, in *Nanozymology*, Springer, Berlin **2020**, p. 105.
- [83] C. Xu, X. Qu, *NPG Asia Mater.* **2014**, *6*, e90.
- [84] W. Zhu, Z. Dong, T. Fu, J. Liu, Q. Chen, Y. Li, R. Zhu, L. Xu, Z. Liu, *Adv. Funct. Mater.* **2016**, *26*, 5490.
- [85] Y.-B. Feng, L. Hong, A.-L. Liu, W.-D. Chen, G.-W. Li, W. Chen, X.-H. Xia, *Int. J. Environ. Sci. Technol.* **2015**, *12*, 653.
- [86] J. Zhou, D. P. Tang, L. Hou, Y. L. Cui, H. F. Chen, G. N. Chen, *Anal. Chim. Acta* **2012**, *751*, 52.
- [87] Y. Jv, B. Li, R. Cao, *Chem. Commun.* **2010**, *46*, 8017.
- [88] J. M. Park, H. W. Jung, Y. W. Chang, H. S. Kim, M. J. Kang, J. C. Pyun, *Int. J. Nanotechnol.* **2016**, *13*, 402.
- [89] Z. Y. Wu, L. G. Chen, G. L. Shen, R. Q. Yu, *Sens. Actuators, B* **2006**, *119*, 295.
- [90] G. W. Wu, S. B. He, H. P. Peng, H. H. Deng, A. L. Liu, X. H. Lin, X. H. Xia, W. Chen, *Anal. Chem.* **2014**, *86*, 10955.
- [91] E. Alzahrani, R. A. Ahmed, *Int. J. Electrochem. Sci.* **2016**, *11*, 4712.
- [92] Y. Song, D. Cho, S. Venkateswarlu, M. Yoon, *RSC Adv.* **2017**, *7*, 10592.
- [93] X. Tan, L. Zhang, Q. Tang, G. Zheng, H. Li, *Mikrochim. Acta* **2019**, *186*, 280.
- [94] S. F. Cai, C. Qi, Y. D. Li, Q. S. Han, R. Yang, C. Wang, *J. Mater. Chem. B* **2016**, *4*, 1869.
- [95] L. J. Bai, R. Yuan, Y. Q. Chai, Y. L. Yuan, Y. Zhuo, L. Mao, *Biosens. Bioelectron.* **2011**, *26*, 4331.
- [96] F. Chen, D. Wang, J. Chen, J. Ling, H. Yue, L. Gou, H. Tang, *Sens. Actuators, B* **2020**, *305*, 127472.
- [97] Y. Fan, X. R. Tan, X. Ou, S. H. Chen, S. P. Wei, *Biosens. Bioelectron.* **2017**, *87*, 802.
- [98] L. Guo, H. Zheng, C. Zhang, L. Qu, L. Yu, *Talanta* **2020**, *210*, 120621.
- [99] Y. Lu, W. C. Ye, Q. Yang, J. Yu, Q. Wang, P. P. Zhou, C. M. Wang, D. S. Xue, S. Q. Zhao, *Sens. Actuators, B* **2016**, *230*, 721.
- [100] L. Liu, Y. Shi, Y. F. Yang, M. L. Li, Y. J. Long, Y. M. Huang, H. Z. Zheng, *Chem. Commun.* **2016**, *52*, 13912.
- [101] L. Liu, Y. Shi, M. L. Li, C. Q. Sun, Y. J. Long, H. Z. Zheng, *Mol. Catal.* **2017**, *439*, 186.
- [102] Y. Tao, E. Ju, J. Ren, X. Qu, *Chem. Commun.* **2014**, *50*, 3030.
- [103] M. Yin, Z. Duan, C. Zhang, L. Feng, Y. Wan, Y. Cai, H. Liu, S. Li, H. Wang, *Microchem. J.* **2019**, *145*, 864.
- [104] Y. Zhang, P. Sun, L. Zhang, Z. Wang, F. Wang, K. Dong, Z. Liu, J. Ren, X. Qu, *Adv. Funct. Mater.* **2019**, *29*, 1808594.
- [105] Q. Liu, R. Zhu, H. Du, H. Li, Y. Yang, Q. Jia, B. Bian, *Mater. Sci. Eng., C* **2014**, *43*, 321.
- [106] P. Ling, S. Cheng, N. Chen, C. Qian, F. Gao, *ACS Appl. Mater. Interfaces* **2020**, *12*, 17185.
- [107] C. Cui, Q. Wang, Q. Liu, X. Deng, T. Liu, D. Li, X. Zhang, *Sens. Actuators, B* **2018**, *277*, 86.
- [108] Y. Huang, M. Zhao, S. Han, Z. Lai, J. Yang, C. Tan, Q. Ma, Q. Lu, J. Chen, X. Zhang, Z. Zhang, B. Li, B. Chen, Y. Zong, H. Zhang, *Adv. Mater.* **2017**, *29*, 1700102.
- [109] S. Xie, J. Ye, Y. Yuan, Y. Chai, R. Yuan, *Nanoscale* **2015**, *7*, 18232.
- [110] L. Mi, Y. Sun, L. Shi, T. Li, *ACS Appl. Mater. Interfaces* **2020**, *12*, 7879.
- [111] J. Wang, X. Yang, T. Wei, J. Bao, Q. Zhu, Z. Dai, *ACS Appl. Bio Mater.* **2018**, *1*, 382.
- [112] X. Deng, Y. Fang, S. Lin, Q. Cheng, Q. Liu, X. Zhang, *ACS Appl. Mater. Interfaces* **2017**, *9*, 3514.
- [113] J. He, F. Xu, J. Hu, S. Wang, X. Hou, Z. Long, *Microchem. J.* **2017**, *135*, 91.
- [114] L. Su, Z. Zhang, Y. Xiong, *Nanoscale* **2018**, *10*, 20120.
- [115] W. Li, Y. Li, H.-L. Qian, X. Zhao, C.-X. Yang, X.-P. Yan, *Talanta* **2019**, *204*, 224.
- [116] J. Xi, G. Wei, L. An, Z. Xu, Z. Xu, L. Fan, L. Gao, *Nano Lett.* **2019**, *19*, 7645.
- [117] H. Wu, F. Li, W. Shao, J. Gao, D. Ling, *ACS Cent. Sci.* **2019**, *5*, 477.
- [118] L. Huang, D. W. Sun, H. Pu, Q. Wei, *Compr. Rev. Food Sci.: Food Saf.* **2019**, *18*, 1496.
- [119] Y. Dai, S. Cheng, Z. Wang, R. Zhang, Z. Yang, J. Wang, B. C. Yung, Z. Wang, O. Jacobson, C. Xu, Q. Ni, G. Yu, Z. Zhou, X. Chen, *ACS Nano* **2018**, *12*, 455.
- [120] T. R. Hoare, D. S. Kohane, *Polymer* **2008**, *49*, 1993.
- [121] J. Li, D. J. Mooney, *Nat. Rev. Mater.* **2016**, *1*, 16071.
- [122] X. Zhao, B. Guo, H. Wu, Y. Liang, P. X. Ma, *Nat. Commun.* **2018**, *9*, 2784.
- [123] X. Liu, J. Liu, S. Lin, X. Zhao, *Mater. Today* **2020**, *36*, 102.
- [124] L. Ma, X. Feng, H. Liang, K. Wang, Y. Song, L. Tan, B. Wang, R. Luo, Z. Liao, G. Li, X. Liu, S. Wu, C. Yang, *Mater. Today* **2020**, *36*, 48.
- [125] V. Pertici, C. Pin-Barre, C. Rivera, C. Pellegrino, J. Laurin, D. Gigmes, T. Trimaille, *Biomacromolecules* **2019**, *20*, 149.
- [126] R. Narayanaswamy, V. P. Torchilin, *Molecules* **2019**, *24*, 603.
- [127] A. Vashist, A. Vashist, Y. K. Gupta, S. Ahmad, *J. Mater. Chem. B* **2014**, *2*, 147.
- [128] Z. Deng, T. Hu, Q. Lei, J. He, P. X. Ma, B. Guo, *ACS Appl. Mater. Interfaces* **2019**, *11*, 6796.
- [129] G.-L. Ying, N. Jiang, S. Maharjan, Y.-X. Yin, R.-R. Chai, X. Cao, J.-Z. Yang, A. K. Miri, S. Hassan, Y. S. Zhang, *Adv. Mater.* **2018**, *30*, 1805460.
- [130] Y. Sang, W. Li, H. Liu, L. Zhang, H. Wang, Z. Liu, J. Ren, X. Qu, *Adv. Funct. Mater.* **2019**, *29*, 1900518.
- [131] J. Xi, Q. Wu, Z. Xu, Y. Wang, B. Zhu, L. Fan, L. Gao, *ACS Biomater. Sci. Eng.* **2018**, *4*, 4391.
- [132] L. Li, B. Xiao, J. Mu, Y. Zhang, C. Zhang, H. Cao, R. Chen, H. K. Patra, B. Yang, S. Feng, Y. Tabata, N. K. H. Slater, J. Tang, Y. Shen, J. Gao, *ACS Nano* **2019**, *13*, 14283.
- [133] J. Chen, S. Li, Y. Zhang, W. Wang, X. Zhang, Y. Zhao, Y. Wang, H. Bi, *Adv. Healthcare Mater.* **2017**, *6*, 1700746.
- [134] Z. Zhang, C. He, X. Chen, *Mater. Chem. Front.* **2018**, *2*, 1765.
- [135] S. Yu, S. Wei, L. Liu, D. Qi, J. Wang, G. Chen, W. He, C. He, X. Chen, Z. Gu, *Macromol. Biosci.* **2019**, *7*, 860.
- [136] L. Liu, Y. Zhang, S. Yu, Z. Zhang, C. He, X. Chen, *Macromol. Biosci.* **2018**, *19*, 2123.
- [137] S. Yu, C. Wang, J. Yu, J. Wang, Y. Lu, Y. Zhang, X. Zhang, Q. Hu, W. Sun, C. He, X. Chen, Z. Gu, *Adv. Mater.* **2018**, *30*, 1801527.
- [138] D. Zhang, B. Wang, Y. Sun, C. Wang, S. Mukherjee, C. Yang, Y. Chen, *Macromol. Biosci.* **2020**, *20*, 2000036.
- [139] F. Ullah, M. B. H. Othman, F. Javed, Z. Ahmad, H. M. Akil, *Mater. Sci. Eng., C* **2015**, *57*, 414.
- [140] K. Varaprasad, G. M. Raghavendra, T. Jayaramudu, M. M. Yallapu, R. Sadiku, *Mater. Sci. Eng., C* **2017**, *79*, 958.
- [141] T. Nochi, Y. Yuki, H. Takahashi, S.-i. Sawada, M. Mejima, T. Kohda, N. Harada, I. G. Kong, A. Sato, N. Kataoka, D. Tokuhara,

- S. Kurokawa, Y. Takahashi, H. Tsukada, S. Kozaki, K. Akiyoshi, H. Kiyono, *Nat. Mater.* **2010**, 9, 572.
- [142] Y. Liu, J. Du, M. Yan, M. Y. Lau, J. Hu, H. Han, O. O. Yang, S. Liang, W. Wei, H. Wang, J. Li, X. Zhu, L. Shi, W. Chen, C. Ji, Y. Lu, *Nat. Nanotechnol.* **2013**, 8, 187.
- [143] Q. Wang, J. L. Mynar, M. Yoshida, E. Lee, M. Lee, K. Okuro, K. Kinbara, T. Aida, *Nature* **2010**, 463, 339.
- [144] L. Jiao, J. Y. R. Seow, W. S. Skinner, Z. U. Wang, H.-L. Jiang, *Mater. Today* **2019**, 27, 43.
- [145] X. Fan, F. Yang, J. Huang, Y. Yang, C. Nie, W. Zhao, L. Ma, C. Cheng, C. Zhao, R. Haag, *Nano Lett.* **2019**, 19, 5885.
- [146] Y. Yang, Y. Deng, J. Huang, X. Fan, C. Cheng, C. Nie, L. Ma, W. Zhao, C. Zhao, *Adv. Funct. Mater.* **2019**, 29, 1900143.
- [147] W. Cai, C.-C. Chu, G. Liu, Y.-X. J. Wang, *Small* **2015**, 11, 4806.
- [148] Y. Liu, Y. Cheng, H. Zhang, M. Zhou, Y. Yu, S. Lin, B. Jiang, X. Zhao, L. Miao, C.-W. Wei, Q. Liu, Y.-W. Lin, Y. Du, C. J. Butch, H. Wei, *Sci. Adv.* **2020**, 6, eabb2695.
- [149] H. Liang, F. Lin, Z. Zhang, B. Liu, S. Jiang, Q. Yuan, J. Liu, *ACS Appl. Mater. Interfaces* **2017**, 9, 1352.
- [150] M. B. Majewski, A. J. Howarth, P. Li, M. R. Wasielewski, J. T. Hupp, O. K. Farha, *CrystEngComm* **2017**, 19, 4082.
- [151] J. Yu, C. Mu, B. Yan, X. Qin, C. Shen, H. Xue, H. Pang, *Mater. Horiz.* **2017**, 4, 557.
- [152] H. Li, H. Liu, J. Zhang, Y. Cheng, C. Zhang, X. Fei, Y. Xian, *ACS Appl. Mater. Interfaces* **2017**, 9, 40716.
- [153] D. Yu, M. Ma, Z. Liu, Z. Pi, X. Du, J. Ren, X. Qu, *Biomaterials* **2020**, 255, 120160.
- [154] Z. W. Jiang, F. Q. Dai, C. Z. Huang, Y. F. Li, *RSC Adv.* **2016**, 6, 86443.
- [155] F. Ke, L.-G. Qiu, J. Zhu, *Nanoscale* **2014**, 6, 1596.
- [156] X. Qian Tang, Y. Dan Zhang, Z. Wei Jiang, D. Mei Wang, C. Zhi Huang, Y. Fang Li, *Talanta* **2018**, 179, 43.
- [157] A. M. Wright, Z. Wu, G. Zhang, J. L. Mancuso, R. J. Comito, R. W. Day, C. H. Hendon, J. T. Miller, M. Dincă, *Chem* **2018**, 4, 2894.
- [158] Z. Tian, K. Yang, T. Yao, X. Li, Y. Ma, C. Qu, X. Qu, Y. Xu, Y. Guo, Y. Qu, *Small* **2019**, 15, 1903746.
- [159] P. Li, Q. Chen, T. C. Wang, N. A. Vermeulen, B. L. Mehdi, A. Dohnalkova, N. D. Browning, D. Shen, R. Anderson, D. A. Gómez-Gualdrón, F. M. Cetin, J. Jagiello, A. M. Asiri, J. F. Stoddart, O. K. Farha, *Chem* **2018**, 4, 1022.
- [160] L. Gao, K. M. Giglio, J. L. Nelson, H. Sondermann, A. J. Travis, *Nanoscale* **2014**, 6, 2588.
- [161] X. Liu, Z. Yan, Y. Zhang, Z. Liu, Y. Sun, J. Ren, X. Qu, *ACS Nano* **2019**, 13, 5222.
- [162] L. Zhang, Y. Zhang, Z. Wang, F. Cao, Y. Sang, K. Dong, F. Pu, J. Ren, X. Qu, *Mater. Horiz.* **2019**, 6, 1682.
- [163] H. Ejima, J. J. Richardson, K. Liang, J. P. Best, M. P. van Koeven, G. K. Such, J. Cui, F. Caruso, *Science* **2013**, 341, 154.
- [164] J. Guo, Y. Ping, H. Ejima, M. Alt, M. Meissner, J. J. Richardson, Y. Yan, K. Peter, D. von Elverfeldt, C. E. Hagemeyer, F. Caruso, *Angew. Chem., Int. Ed.* **2014**, 53, 5546.
- [165] M. A. Rahim, M. Björnalm, T. Suma, M. Faria, Y. Ju, K. Kempe, M. Müller, H. Ejima, A. D. Stickland, F. Caruso, *Angew. Chem., Int. Ed.* **2016**, 55, 13803.
- [166] Y. Ping, J. Guo, H. Ejima, X. Chen, J. J. Richardson, H. Sun, F. Caruso, *Small* **2015**, 11, 2032.
- [167] X. Li, P. Gao, J. Tan, K. Xiong, M. F. Maitz, C. Pan, H. Wu, Y. Chen, Z. Yang, N. Huang, *ACS Appl. Mater. Interfaces* **2018**, 10, 40844.
- [168] Q. Tu, X. Shen, Y. Liu, Q. Zhang, X. Zhao, M. F. Maitz, T. Liu, H. Qiu, J. Wang, N. Huang, Z. Yang, *Mater. Chem. Front.* **2019**, 3, 265.
- [169] Y. Dai, Z. Yang, S. Cheng, Z. Wang, R. Zhang, G. Zhu, Z. Wang, B. C. Yung, R. Tian, O. Jacobson, C. Xu, Q. Ni, J. Song, X. Sun, G. Niu, X. Chen, *Adv. Mater.* **2018**, 30, 1704877.
- [170] L. Zhang, S. S. Wan, C. X. Li, L. Xu, H. Cheng, X. Z. Zhang, *Nano Lett.* **2018**, 18, 7609.
- [171] D.-W. Zheng, Q. Lei, J.-Y. Zhu, J.-X. Fan, C.-X. Li, C. Li, Z. Xu, S.-X. Cheng, X.-Z. Zhang, *Nano Lett.* **2017**, 17, 284.
- [172] Q. Sun, C.-W. Fu, B. Aguila, J. Perman, S. Wang, H.-Y. Huang, F.-S. Xiao, S. Ma, *J. Am. Chem. Soc.* **2018**, 140, 984.
- [173] T. Liu, J. Tian, L. Cui, Q. Liu, L. Wu, X. Zhang, *Colloids Surf., B* **2019**, 178, 137.
- [174] X. Fan, R. Tian, T. Wang, S. Liu, L. Wang, J. Xu, J. Liu, M. Ma, Z. Wu, *Nanoscale* **2018**, 10, 22155.
- [175] Y. Su, D. Wu, J. Chen, G. Chen, N. Hu, H. Wang, P. Wang, H. Han, G. Li, Y. Wu, *Anal. Chem.* **2019**, 91, 11687.
- [176] Y. Xiong, Y. Qin, L. Su, F. Ye, *Chem. - Eur. J.* **2017**, 23, 11037.
- [177] H. Yan, D. Shao, Y.-H. Lao, M. Li, H. Hu, K. W. Leong, *Adv. Sci.* **2019**, 6, 1900605.
- [178] R. H. Fang, A. V. Kroll, W. Gao, L. Zhang, *Adv. Mater.* **2018**, 30, 1706759.
- [179] Z. Wang, F. Zhang, D. Shao, Z. Chang, L. Wang, H. Hu, X. Zheng, X. Li, F. Chen, Z. Tu, M. Li, W. Sun, L. Chen, W.-F. Dong, *Adv. Sci.* **2019**, 6, 1901690.
- [180] X. Pang, X. Liu, Y. Cheng, C. Zhang, E. Ren, C. Liu, Y. Zhang, J. Zhu, X. Chen, G. Liu, *Adv. Mater.* **2019**, 31, 1902530.
- [181] S. Amor, F. Puentes, D. Baker, P. van der Valk, *Immunology* **2010**, 129, 154.
- [182] M. T. Herrero, C. Estrada, L. Maatouk, S. Vyas, *Front. Neuroanat.* **2015**, 9, 32.
- [183] Y. Zhao, M. J. Haney, V. Mahajan, B. C. Reiner, A. Dunaevsky, R. L. Mosley, A. V. Kabanov, H. E. Gendelman, E. V. Batrakova, *J. Nanomed. Nanotechnol.* **2011**, S4, 003.
- [184] S. Zanganeh, R. Spitler, G. Hutter, J. Q. Ho, M. Pauliah, M. Mahmoudi, *Immunotherapy* **2017**, 9, 819.
- [185] S.-K. Baek, A. R. Makkouk, T. Krasieva, C.-H. Sun, S. J. Madsen, H. Hirschberg, *J. Neuro-Oncol.* **2011**, 104, 439.
- [186] E. G. Rosenbaum, J. W. Roat, L. Gao, R. F. Yang, D. S. Manickam, J. X. Yin, H. D. Schultz, T. K. Bronich, E. V. Batrakova, A. V. Kabanov, I. H. Zucker, M. C. Zimmerman, *Biomaterials* **2010**, 31, 5218.
- [187] M. J. Haney, Y. Zhao, S. Li, S. M. Higginbotham, S. L. Booth, H. Y. Han, J. A. Vetro, R. L. Mosley, A. V. Kabanov, H. E. Gendelman, E. V. Batrakova, *Nanomedicine* **2011**, 6, 1215.
- [188] N. L. Klyachko, D. S. Manickam, A. M. Brynskikh, S. V. Uglanova, S. Li, S. M. Higginbotham, T. K. Bronich, E. V. Batrakova, A. V. Kabanov, *Nanomedicine* **2012**, 8, 119.
- [189] A. M. Brynskikh, Y. Zhao, R. L. Mosley, S. Li, M. D. Boska, N. L. Klyachko, A. V. Kabanov, H. E. Gendelman, E. V. Batrakova, *Nanomedicine* **2010**, 5, 379.
- [190] E. V. Batrakova, S. Li, A. D. Reynolds, R. L. Mosley, T. K. Bronich, A. V. Kabanov, H. E. Gendelman, *Bioconjug. Chem.* **2007**, 18, 1498.
- [191] N. L. Klyachko, M. J. Haney, Y. Zhao, D. S. Manickam, V. Mahajan, P. Suresh, S. D. Hingtgen, R. L. Mosley, H. E. Gendelman, A. V. Kabanov, E. V. Batrakova, *Nanomedicine* **2014**, 9, 1403.
- [192] Y. Zhao, M. J. Haney, N. L. Klyachko, S. Li, S. L. Booth, S. M. Higginbotham, J. Jones, M. C. Zimmerman, R. L. Mosley, A. V. Kabanov, H. E. Gendelman, E. V. Batrakova, *Nanomedicine* **2011**, 6, 25.
- [193] D. S. Manickam, A. M. Brynskikh, J. L. Kopanic, P. L. Sorgen, N. L. Klyachko, E. V. Batrakova, T. K. Bronich, A. V. Kabanov, *J. Controlled Release* **2012**, 162, 636.
- [194] H. Min, J. Wang, Y. Qi, Y. Zhang, X. Han, Y. Xu, J. Xu, Y. Li, L. Chen, K. Cheng, G. Liu, N. Yang, Y. Li, G. Nie, *Adv. Mater.* **2019**, 31, 1808200.
- [195] R. Li, Y. He, S. Zhang, J. Qin, J. Wang, *Acta Pharm. Sin. B* **2018**, 8, 14.
- [196] V. Vijayan, S. Uthaman, I.-K. Park, *Polymers* **2018**, 10, 983.
- [197] S. Tan, T. Wu, D. Zhang, Z. Zhang, *Theranostics* **2015**, 5, 863.
- [198] R. H. Fang, C.-M. J. Hu, B. T. Luk, W. Gao, J. A. Copp, Y. Tai, D. E. O'Connor, L. Zhang, *Nano Lett.* **2014**, 14, 2181.

- [199] Z. Chai, X. Hu, W. Lu, *Sci. China Mater.* **2017**, 60, 504.
- [200] Z. Yu, P. Zhou, W. Pan, N. Li, B. Tang, *Nat. Commun.* **2018**, 9, 5044.
- [201] M. Z. Alyami, S. K. Alsaiani, Y. Li, S. S. Qutub, F. A. Aleisa, R. Sougrat, J. S. Merzaban, N. M. Khashab, *J. Am. Chem. Soc.* **2020**, 142, 1715.
- [202] C. M. J. Hu, L. Zhang, S. Aryal, C. Cheung, R. H. Fang, L. Zhang, *Proc. Natl. Acad. Sci. USA* **2011**, 108, 10980.
- [203] H. Ding, Y. Cai, L. Gao, M. Liang, B. Miao, H. Wu, Y. Liu, N. Xie, A. Tang, K. Fan, X. Yan, G. Nie, *Nano Lett.* **2019**, 19, 203.
- [204] C.-M. J. Hu, R. H. Fang, L. Zhang, *Adv. Healthcare Mater.* **2012**, 1, 537.
- [205] X. Yang, Y. Yang, F. Gao, J. J. Wei, C. G. Qian, M. J. Sun, *Nano Lett.* **2019**, 19, 4334.
- [206] Y. Wang, Z. Liu, H. Wang, Z. Meng, Y. Wang, W. Miao, X. Li, H. Ren, *Acta Biomater.* **2019**, 92, 241.
- [207] L. Sercombe, T. Veerati, F. Moheimani, S. Y. Wu, A. K. Sood, S. Hua, *Front. Pharmacol.* **2015**, 6, 286.
- [208] T. O. B. Olusanya, R. R. Haj Ahmad, D. M. Ibegbu, J. R. Smith, A. A. Elkordy, *Molecules* **2018**, 23, 907.
- [209] M. de Smet, E. Heijman, S. Langereis, N. M. Hijnen, H. Grull, *J. Controlled Release* **2011**, 150, 102.
- [210] M. de Smet, S. Langereis, S. v. den Bosch, H. Grull, *J. Controlled Release* **2010**, 143, 120.
- [211] X. Song, J. Xu, C. Liang, Y. Chao, Q. Jin, C. Wang, M. Chen, Z. Liu, *Nano Lett.* **2018**, 18, 6360.
- [212] O. A. Kost, O. V. Beznos, N. G. Davydova, D. S. Manickam, Nikolskaya, A. E. Guller, P. V. Binevski, N. B. Chesnokova, A. B. Shekhter, N. L. Klyachko, A. V. Kabanov, *Oxid. Med. Cell. Longevity* **2015**, 2015, 5194239.
- [213] Y. Jiang, P. Arounleut, S. Rheiner, Y. Bae, A. V. Kabanov, C. Milligan, D. S. Manickam, *J. Controlled Release* **2016**, 231, 38.
- [214] M. Zhang, X. Zang, M. Wang, Z. Li, M. Qiao, H. Hu, D. Chen, *J. Mater. Chem. B* **2019**, 7, 2421.
- [215] S. G. Antimisariar, S. Mourtas, A. Marazioti, *Pharmaceutics* **2018**, 10, 218.
- [216] M. J. Haney, N. L. Klyachko, Y. Zhao, R. Gupta, E. G. Plotnikova, Z. He, T. Patel, A. Piroyan, M. Sokolsky, A. V. Kabanov, E. V. Batrakova, *J. Controlled Release* **2015**, 207, 18.
- [217] Y. T. Sato, K. Umezaki, S. Sawada, S.-a. Mukai, Y. Sasaki, N. Harada, H. Shiku, K. Akiyoshi, *Sci. Rep.* **2016**, 6, 21933.
- [218] D. Wang, H. Dong, M. Li, Y. Cao, F. Yang, K. Zhang, W. Dai, C. Wang, X. Zhang, *ACS Nano* **2018**, 12, 5241.
- [219] D. Dehaini, X. Wei, R. H. Fang, S. Masson, P. Angsantikul, B. T. Luk, Y. Zhang, M. Ying, Y. Jiang, A. V. Kroll, W. Gao, L. Zhang, *Adv. Mater.* **2017**, 29, 1606209.
- [220] S. Gao, H. Lin, H. Zhang, H. Yao, Y. Chen, J. Shi, *Adv. Sci.* **2019**, 6, 1801733.
- [221] H. A. Rather, R. Thakore, R. Singh, D. Jhala, S. Singh, R. Vasita, *Bioact. Mater.* **2018**, 3, 201.
- [222] J. Zhao, W. Gao, X. Cai, J. Xu, D. Zou, Z. Li, B. Hu, Y. Zheng, *Theranostics* **2019**, 9, 2843.
- [223] J. Jiang, C. He, S. Wang, H. Jiang, J. Li, L. Li, *Carbohydr. Polym.* **2018**, 198, 348.
- [224] C. Cheng, J. Zhang, S. Li, Y. Xia, C. Nie, Z. Shi, J. L. Cuellar-Camacho, N. Ma, R. Haag, *Adv. Mater.* **2018**, 30, 1705452.
- [225] Y. Xia, S. Li, C. Nie, J. Zhang, S. Zhou, H. Yang, M. Li, W. Li, C. Cheng, R. Haag, *Appl. Mater. Today* **2019**, 16, 518.
- [226] Z. Li, X. Yang, Y. Yang, Y. Tan, Y. He, M. Liu, X. Liu, Q. Yuan, *Chem. - Eur. J.* **2018**, 24, 409.
- [227] F. Li, Y. Qiu, F. Xia, H. Sun, H. Liao, A. Xie, J. Lee, P. Lin, M. Wei, Y. Shao, B. Yang, Q. Weng, D. Ling, *Nano Today* **2020**, 35, 100925.
- [228] S. Kango, S. Kalia, A. Celli, J. Njuguna, Y. Habibi, R. Kumar, *Prog. Polym. Sci.* **2013**, 38, 1232.
- [229] G. Kickelbick, *Prog. Polym. Sci.* **2003**, 28, 83.
- [230] P. Mansky, Y. Liu, E. Huang, T. Russell, C. Hawker, *Science* **1997**, 275, 1458.
- [231] L. Gao, M. Li, S. Ehrmann, Z. Tu, R. Haag, *Angew. Chem., Int. Ed.* **2019**, 58, 3645.
- [232] Z. Tang, C. He, H. Tian, J. Ding, B. S. Hsiao, B. Chu, X. Chen, *Prog. Polym. Sci.* **2016**, 60, 86.
- [233] Q. Gao, P. Li, H. Zhao, Y. Chen, L. Jiang, P. X. Ma, *Polym. Chem.* **2017**, 8, 6386.
- [234] C. Zeng, N. Lu, Y. Wen, G. Liu, R. Zhang, J. Zhang, F. Wang, X. Liu, Q. Li, Z. Tang, M. Zhang, *ACS Appl. Mater. Interfaces* **2019**, 11, 1790.
- [235] Y. Liu, Y. Xiang, D. Ding, R. Guo, *RSC Adv.* **2016**, 6, 112435.
- [236] M. Yan, G. Chen, Y. She, J. Ma, S. Hong, Y. Shao, A. M. Abd El-Aty, M. Wang, S. Wang, J. Wang, *J. Agric. Food Chem.* **2019**, 67, 9658.
- [237] Y. Chen, L. Yu, B. Zhang, W. Feng, M. Xu, L. Gao, N. Liu, Q. Wang, X. Huang, P. Li, W. Huang, *Biomacromolecules* **2019**, 20, 2230.
- [238] Z. Chen, J.-J. Yin, Y.-T. Zhou, Y. Zhang, L. Song, M. Song, S. Hu, N. Gu, *ACS Nano* **2012**, 6, 4001.
- [239] W. He, Y.-T. Zhou, W. G. Wamer, X. Hu, X. Wu, Z. Zheng, M. D. Boudreau, J.-J. Yin, *Biomaterials* **2013**, 34, 765.
- [240] M. Drozd, M. Pietrzak, P. Parzuchowski, M. Mazurkiewicz-Pawlacka, E. Malinowska, *Nanotechnology* **2015**, 26, 495101.
- [241] Y. Zhang, F. Wang, C. Liu, Z. Wang, L. Kang, Y. Huang, K. Dong, J. Ren, X. Qu, *ACS Nano* **2018**, 12, 651.
- [242] E. L. Siegler, Y. J. Kim, P. Wang, *J. Cell. Immunother.* **2016**, 2, 69.
- [243] S. Neri, S. Garcia Martin, C. Pezzato, L. J. Prins, *J. Am. Chem. Soc.* **2017**, 139, 1794.
- [244] A. Gupta, R. Das, G. Yesilbag Tonga, T. Mizuhara, V. M. Rotello, *ACS Nano* **2018**, 12, 89.
- [245] W. Yin, J. Yu, F. Lv, L. Yan, L. R. Zheng, Z. Gu, Y. Zhao, *ACS Nano* **2016**, 10, 11000.
- [246] D. Lauster, M. Glanz, M. Bardua, K. Ludwig, M. Hellmund, U. Hoffmann, A. Hamann, C. Böttcher, R. Haag, C. P. R. Hackenberger, A. Herrmann, *Angew. Chem., Int. Ed.* **2017**, 56, 5931.
- [247] X. Zheng, Q. Liu, C. Jing, Y. Li, D. Li, W. Luo, Y. Wen, Y. He, Q. Huang, Y.-T. Long, C. Fan, *Angew. Chem., Int. Ed.* **2011**, 50, 11994.
- [248] J. Sang, R. Wu, P. Guo, J. Du, S. Xu, J. Wang, *J. Appl. Polym. Sci.* **2016**, 133, 43065.
- [249] L. Zhang, Z. Qi, Y. Zou, J. Zhang, W. Xia, R. Zhang, Z. He, X. Cai, Y. Lin, S. Z. Duan, J. Li, L. Wang, N. Lu, Z. Tang, *ACS Appl. Mater. Interfaces* **2019**, 11, 30640.
- [250] K. Fan, C. Cao, Y. Pan, D. Lu, D. Yang, J. Feng, L. Song, M. Liang, X. Yan, *Nat. Nanotechnol.* **2012**, 7, 459.
- [251] Y.-H. Zhang, W.-X. Qiu, M. Zhang, L. Zhang, X.-Z. Zhang, *ACS Appl. Mater. Interfaces* **2018**, 10, 15030.
- [252] H. Zhu, J. Li, X. Qi, P. Chen, K. Pu, *Nano Lett.* **2018**, 18, 586.
- [253] K. Müller, E. Bugnicourt, M. Latorre, M. Jorda, Y. Echegoyen Sanz, J. Lagaron, O. Miesbauer, A. Bianchin, S. Hankin, U. Böhlz, G. Pérez, M. Jesdinszki, M. Lindner, Z. Scheuerer, S. Castelló, M. Schmid, *Nanomaterials* **2017**, 7, 74.
- [254] H. Liang, B. Liu, Q. Yuan, J. Liu, *ACS Appl. Mater. Interfaces* **2016**, 8, 15615.
- [255] C. Hou, Q. Luo, J. Liu, L. Miao, C. Zhang, Y. Gao, X. Zhang, J. Xu, Z. Dong, J. Liu, *ACS Nano* **2012**, 6, 8692.
- [256] H. Sun, L. Miao, J. Li, S. Fu, G. An, C. Si, Z. Dong, Q. Luo, S. Yu, J. Xu, J. Liu, *ACS Nano* **2015**, 9, 5461.
- [257] S. Vyas, E. Zaganjor, M. C. Haigis, *Cell* **2016**, 166, 555.
- [258] D. C. Wallace, *Nat. Rev. Cancer* **2012**, 12, 685.
- [259] S. S. Sabharwal, P. T. Schumacker, *Nat. Rev. Cancer* **2014**, 14, 709.
- [260] N. Gong, X. Ma, X. Ye, Q. Zhou, X. Chen, X. Tan, S. Yao, S. Huo, T. Zhang, S. Chen, X. Teng, X. Hu, J. Yu, Y. Gan, H. Jiang, J. Li, X. J. Liang, *Nat. Nanotechnol.* **2019**, 14, 379.
- [261] R. Das, R. F. Landis, G. Y. Tonga, R. Cao-Milan, D. C. Luther, V. M. Rotello, *ACS Nano* **2019**, 13, 229.
- [262] N. Gao, K. Dong, A. Zhao, H. Sun, Y. Wang, J. Ren, X. Qu, *Nano Res.* **2016**, 9, 1079.



- [263] J. Kim, H. Y. Kim, S. Y. Song, S. H. Go, H. S. Sohn, S. Baik, M. Soh, K. Kim, D. Kim, H. C. Kim, N. Lee, B. S. Kim, T. Hyeon, *ACS Nano* **2019**, *13*, 3206.
- [264] C. Nie, M. Stadtmüller, H. Yang, Y. Xia, T. Wolff, C. Cheng, R. Haag, *Nano Lett.* **2020**, *20*, 5367.
- [265] W. Yue, L. Chen, L. Yu, B. Zhou, H. Yin, W. Ren, C. Liu, L. Guo, Y. Zhang, L. Sun, K. Zhang, H. Xu, Y. Chen, *Nat. Commun.* **2019**, *10*, 2025.
- [266] L. Wang, B. Zhu, J. Huang, X. Xiang, Y. Tang, L. Ma, F. Yan, C. Cheng, L. Qiu, *J. Mater. Chem. B* **2020**, *8*, 5245.



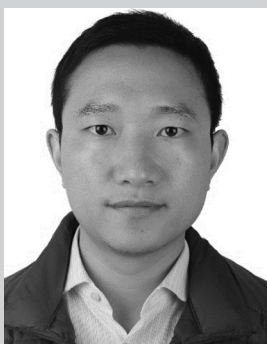
**Sujiao Cao** is now a postdoctoral research fellow at West China Hospital, Sichuan University. She obtained his B.Sc. and Ph.D. degrees from Zhengzhou University and Sichuan University, respectively. Her current research interests include the design and fabrication of biopolymers functionalized or enzyme-mimetic, nanomedicines, nanocatalytic biomaterials, and their applications in diagnosis and therapies for the biomedical fields, such as wound healing, skin tumor, and stem cells regenerations.



**Hongrong Luo** is currently an associate professor in National Engineering Research Center for Biomaterials. She received her Ph.D. from Sichuan University, China. After a postdoc research stay (2008–2011) at National Engineering Research Center for Biomaterials. She moved to the University of California, San Diego, School of Medicine as a postdoc from 2012 and then American Veterans Medical System (VA), San Diego hospital as a research fellow from 2015. Her current research interests include the gene and neural stem cell therapy, implantable scaffolds, and tissue regeneration, and neural electrode and biosensors.



**Li Qiu** is currently a full professor and the Head of Musculoskeletal Ultrasound Diagnosis Group in West China Hospital, Sichuan University. She received her Ph.D. in 2011 for Imaging Medicine and Nuclear Medicine from West China Hospital, Sichuan University. Her current scientific interests are designing new nanomedical imaging, nanomedicines, and enzyme-mimetic biomaterials and exploring their applications in diagnosis and therapies for the biomedical fields, such as wound healing, skin tumor, neural regeneration, and rheumatoid arthritis.



**Chong Cheng** is currently a full professor and the head of the Advanced Low-Dimensional Materials Group in the College of Polymer Science and Engineering at Sichuan University. He obtained his B.Sc. and Ph.D. from Sichuan University. After a research stay at the University of Michigan, Ann Arbor, he joined the Freie Universität Berlin as an AvH research fellow. His current scientific interests include the chemistry, nanostructured design, and nanocatalytic applications of advanced low-dimensional materials for nanomedicines, stem cell scaffolds, electrocatalysts, and energy storage devices, especially the cutting-edge applications of metal–organic frameworks and emerging 2D materials.